NTNU
Norwegian University of
Science and Technology

The Quark-meson model in a magnetic field

Sigurd Loe Grøver

Master of Science in Physics and Mathematics
Submission date: September 2017
Supervisor: Jens Oluf Andersen, IFY

Norwegian University of Science and Technology
Department of Physics

Sigurd Loe Grøver

Abstract

In this thesis we study the chiral phase transition of two-flavor QCD, through the use of the quark-meson model. The effect of a magnetic field on the transition is studied, at finite temperature and baryon chemical potential. The first few sections of the text are devoted to a short introduction to QCD and its thermodynamics, followed by derivations of the free energy of the free complex scalar field and the free fermion field. The quark-meson model is then introduced, and its effective potential computed to one-loop order. The parameters of the model are matched to physical observables taking loop corrections into account. Finally, numerical results are presented. The results are in line with predictions from other effective models, however, they diverge from current lattice results on the topic of magnetic catalysis.

Contents

Notation and Conventions

- The Minkowski metric is $\eta^{\mu\nu} = \text{diag}(1,-1,-1,-1)$.
- The Einstein summation convention is used, where one upper and one lower Greek index imply summation with the Minkowski metric, e.g. $\partial_\mu A^\mu = \eta^{\mu\nu}\partial_\mu A_\nu$.
- Repeated lower Greek indices imply summation with the Euclidean metric $\delta_{\mu\nu}$.
- Repeated Latin indices imply summation of spatial components, e.g. $k_i x_i = \mathbf{k}\cdot\mathbf{x}$.
- Natural units are used, i.e. $k_B = c = \hbar = 1$ where k_B, c and $\hbar$ are the Boltzmann constant, speed of light and reduced Planck constant, respectively.

1. Introduction

This master's thesis is written as a continuation of the work done in the project thesis [1] preceding it. There, the phase diagram of the quark-meson model was studied at finite temperature and baryon chemical potential, in the chiral limit. In this thesis we will expand on those results in a few ways: by incorporating finite pion masses, by adding an external magnetic field, and by taking loop corrections into account when matching the parameters of the model to physical observables.

2. Quantum Chromodynamics

The theory known as Quantum Chromodynamics is regarded as a fundamental theory of the strong interaction. In this section we will give a minimal summary of some of its properties; in particular the symmetries of the theory, which provide the justification for the use of the model which will be studied in the next section.

The building blocks of the theory are quarks, which are fermions, and gluons, which are gauge bosons. The gauge group of QCD is $SU(3)$ (or more generally, $SU(N_c)$ if one allows for an arbitrary number of colors). That is to say, a quark field has three $N_c = 3$ components,

$$\psi = \begin{pmatrix} \psi_1 \\ \psi_2 \\ \psi_3 \end{pmatrix}. \tag{1}$$

The Lagrangian is invariant under global $SU(3)$ transformations on these components, and by introducing a gauge field, the gluon field, it is made to be invariant under local transformations as well. The gluon field has eight components, one for each of the generators of $SU(3)$. There are six different flavors (discovered so far) of quarks, divided into three generations: the up and down quarks are relatively light (their masses are approximately 2 and 5 MeV, respectively), and are the constituents of protons and neutrons. Progressively heavier are the strange, charm, bottom and top quarks, with masses ranging from ~ 95 MeV to ~ 170 GeV [11]. Since the mimimum energy required to create a particle is proportional to its mass, it is possible to neglect the heavier quarks in a low-energy approximation. The (Minkowskian) Lagrangian density of the theory can be written as [12]

$$\mathscr{L}_{\mathrm{QCD}} = \bar{\psi}_i \left[i(\gamma^\mu D_\mu)_{ij} - m\delta_{ij} \right] \psi_j - \frac{1}{4} G^a_{\mu\nu} G^{\mu\nu}_a. \tag{2}$$

Here, the indices i, j correspond to the three components of the quark field. The index a runs from 1 to 8, corresponding to the eight components of the gluon field. D_μ is the covariant derivative

$$(D_\mu)_{ij} = \partial_\mu \delta_{ij} - ig(T_a)_{ij} A^a, \tag{3}$$

with A^a the gluon field, T_a the eight generators of $SU(3)$, and g a dimensionless coupling constant. $G^a_{\mu\nu}$ is the gluon field strength tensor, defined as

$$G^a_{\mu\nu} = \partial_\mu A^a_\nu - \partial_\nu A^a_\mu + g f^{abc} A^b_\mu A^c_\nu, \tag{4}$$

with f^{abc} the structure constants of $SU(3)$, satisfying

$$[T^a, T^b] = f^{abc} T^c. \tag{5}$$

The Lagrangian is invariant under simultaneous transformations

$$\begin{aligned}\psi &\to \mathrm{e}^{i\alpha_a(x)T^a}\psi \\ \bar{\psi} &\to \bar{\psi}\mathrm{e}^{-i\alpha_a(x)T^a} \\ A^a_\mu &\to A^a_\mu - \frac{1}{g}\partial_\mu \alpha^a(x),\end{aligned} \tag{6}$$

where $\alpha(x)$ is an arbitrary phase.

2.1. Color charge, confinement and asymptotic freedom

We can associate a conserved charge with the strong interaction, known as color charge. The three components of the quark field each correspond to one of the colors red, green and blue. Quarks carry one unit of color, whereas antiquarks carry one unit of "anticolor" ("antired", etc.). Gluons carry one unit of color and one unit of anticolor. To get a color-neutral composite, we can either combine one unit of each color ("red + green + blue = white"), or a unit of one color with a unit of the corresponding anticolor. It turns out that QCD has a property known as confinement, which means that quarks and gluons never appear as isolated particles, and are only found in color-neutral bound states. Three quarks make a baryon, such as the proton and neutron, whereas a quark-antiquark pair constitute a meson. This is related to the property known as asymptotic freedom: The coupling between quarks and gluons increases at low energies (i.e. when the center-of-mass energy of two interacting particles is low), and approaches zero as the energy approaches infinity. This means that the attractive force between two quarks in a hadron becomes increasingly strong when the distance between them increases (large distance corresponds to low energy), and an infinite amount of energy would be required to remove a single quark completely from a hadron, or completely separate the quark-antiquark pair in a pion.

Quarks and gluons that exist in bound states make up most of the matter around us. It is thought, however, that at sufficiently high temperatures and /or pressures a phase transition occurs. Quarks cease to be confined to hadrons, and are better described as free particles.

2.2. Flavor symmetry

If we have several quark flavors, the quark field ψ becomes a multiplet,

$$\psi = \begin{pmatrix} u \\ d \\ \vdots \end{pmatrix}, \tag{7}$$

and the mass term in (2) becomes a diagonal matrix of quark masses, $m = \mathrm{diag}(m_u, m_d, \dots,)$. We will be concerned with the low-energy approximation, including only the up and down quarks. In this case, the Lagrangian has an approximate flavor symmetry: if the masses of the up and down quarks were precisely equal, $U(2)$ transformations of the flavor doublet would leave the Lagrangian invariant. There is also an approximate chiral symmetry: We can decompose a fermion field into left-handed and right-handed components, $\psi = \psi_R + \psi_L$, where

$$\begin{aligned}\psi_R &= \frac{1}{2}(1+\gamma_5)\psi, \\ \psi_L &= \frac{1}{2}(1-\gamma_5)\psi.\end{aligned} \tag{8}$$

where $\gamma_5 = \gamma_1\gamma_2\gamma_3\gamma_0$. For massless fermions, these components correspond to particles with positive and negative helicity, respectively [10]. Writing (2) in terms of these components, we have

$$\mathscr{L}_{\text{QCD}} = \bar{\psi}_{Ri} i(\gamma^\mu D_\mu)_{ij} \psi_{Rj} + \bar{\psi}_{Li} i(\gamma^\mu D_\mu)_{ij} \psi_{Lj} - m(\bar{\psi}_{Ri}\psi_{Li} + \bar{\psi}_{Li}\psi_{Ri}) - \frac{1}{4} G^a_{\mu\nu} G^{\mu\nu}_a. \tag{9}$$

If not for the mass term, the chiral components would decouple in the Lagrangian, and we could make $U(2)$ transformations on the chiral components independently. The symmetry group $U(2)_L \times U(2)_R$ can be decomposed into $SU(2)_L \times SU(2)_R \times U(1)_V \times U(1)_A$ (V for vector and A for axial), when the chiral components transform independently under $SU(2)$. Under $U(1)_V$, the fields transform as follows:

$$\psi_L \to e^{i\alpha}\psi_L, \qquad \psi_R \to e^{i\alpha}\psi_R. \tag{10}$$

And under $U(1)_A$,

$$\psi_L \to e^{i\beta}\psi_L, \qquad \psi_R \to e^{-i\beta}\psi_R. \tag{11}$$

The $U(1)_A$ symmetry, while an exact symmetry at the classical level (in the case of vanishing quark masses), turns out not to be an exact symmetry of the quantum field theory due to a so-called anomaly [13]. Therefore, the flavor symmetry group of this model in the limit of vanishing quark masses is $SU(2)_L \times SU(2)_R \times U(1)_V$.

While the masses of the up and down quarks are in reality finite and different, they are small enough to consider chiral symmetry an approximate symmetry of the Lagrangian. As it turns out, this symmetry is spontaneously broken down to $SU(2)_V \times U(1)_V$ in the vacuum by the formation of a quark condensate, a nonzero expectation value $\langle\bar{\psi}\psi\rangle$. According to Goldstone's theorem, there should appear massless bosons in the energy spectrum. They are known as pions. However, since the symmetry which is being broken is not an exact one, the pions are not in fact massless; they do, however have relatively small masses, and are classified as pseudo-Goldstone bosons.

2.3. The phases of QCD

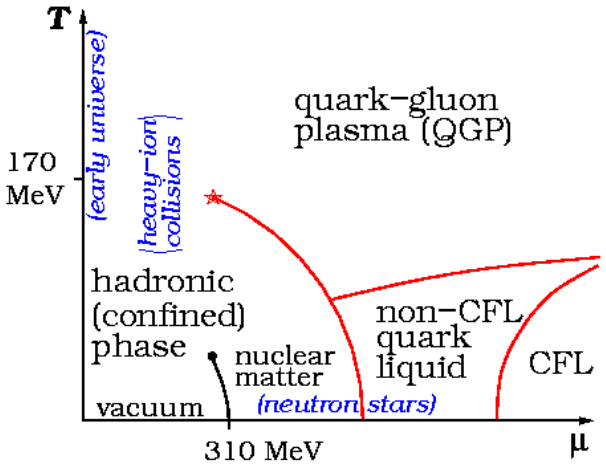

Figure 1: This diagram shows what the qualitative form of the QCD phase diagram, in the plane of temperature and baryon chemical potential, is thought to be, as pieced together by different means of research.

The current understanding of the QCD phase diagram is summarized in figure 1 [14]. At low temperature and quark chemical potential, quarks and gluons are confined in bound states (hadrons), and chiral

symmetry is spontaneously broken. When the temperature increases, the coupling between the particles decreases, and it is expected that a phase transition will occur at some point, leading to a phase known as quark-gluon plasma, where the quarks and gluons are deconfined and asymptotically free, and approximate chiral symmetry is restored. . At low densities (corresponding to low baryon chemical potential), this transition is a crossover, whereas at a sufficiently high density one expects to find a critical point, beyond which the phase transition is discontinuous (first-order). At low temperature and high density, the hadrons become increasingly closely packed together. At sufficiently high densities, the hadrons are expected to merge with a each other, leading to a phase of deconfined quarks and gluons. It is expected that a phase of matter may result in which the quarks form Cooper-pairs, leading to a color-superconducting phase of matter known as the color-flavor-locked (CFL) phase [15]. In the area between the hadronic and CFL phase, several distinct phases of QCD have been hypothesized. This is currently a blooming area of research [2].

It is generally very difficult to treat QCD analytically. Therefore, many of the results on its phase structure are obtained in other ways. An important method is known as lattice QCD, which is a numerical method based on the discretization of spacetime. One of its main limitations, known as the sign problem, makes this method unfeasible at finite baryon chemical potential (although it's possible to make extrapolations to small but finie chemical potentials) [3]. Another approach is the use of effective models. In this thesis we will be concerned with the Quark-meson model, which possesses the same symmetries as QCD itself (although color symmetry is left as a global symmetry). This model is used to investigate the chiral transition of QCD at finite temperature and baryon chemical potential. Another important effective model is the NJL model. In both of these models, the quarks appear as free particles. Both models can be extended, by the inclusion of a Polyakov loop potential, to also model the confinement transition.

In this thesis, much of the focus will be on the behavior of the QM model in the presence of an external magnetic field. The physical relevance of this can be found in a type of neutron star known as magnetars, which harbor extremely strong magnetic fields as well as pressures and temperatures potentially high enough to allow for quark matter; as well as in non-central heavy ion collisions produced in particle accelerators. Finite magnetic fields can be studied using lattice QCD, so this can be used as another way of comparing lattice results with those of effective models.

2.4. QCD in a strong magnetic field

The thermodynamics of quark matter in a strong external magnetic field is interesting for several reasons. For example, non-central heavy ion collisions taking place at particle accelerators may produce fields on the order of $|eB| \sim 15m_\pi^2$ [4]. Furthermore, a type of neutron star known as magnetars harbors extremely strong magnetic fields. The magnetic field strength on the surface of such stars has been determined to be on the order of 10^{11}T, and the field strength in the may be as high as $\sim 10^{14}$ T, or $|eB| \sim 3m_\pi^2$ [5].

The first investigations of the behavior of quark matter in the presence of a strong magnetic field came from the use of effective models such as the quark-meson model and the NJL model. In particular, the chiral transition was studied, and it was found that the introduction of a magnetic field enhances the symmetry breaking - i.e., the transition occurs at higher temperatures and chemical potentials, and the magnitude of the chiral condensate is an increasing function of the magnetic field strength. This is in line with general wisdom from other areas of quantum field theory. The enhancement of dynamical symmetry breaking by an external magnetic field is a well known phenomenon, known as magnetic catalysis. The underlying mechanism is *dimensional reduction*. See ref. [6] for a review of this phenomenon.

However, these results have been contradicted by lattice calculations. It has been found that magnetic catalysis does appear to take place at low temperatures; however, as the temperature increases the

influence of the field strength on the chiral transition becomes more complicated, and at sufficiently high temperatures, one finds *inverse* magnetic catalysis. The magnitude of the chiral condensate is then a decreasing function of the field strength [8]. Attempts to reproduce this behavior by modifying effective models have been unsuccessful so far, see e.g. [9]. It is thought that, while the mechanism of magnetic catalysis is present, a competing mechanism, not captured by the effective models, pushes the condensate in the opposite direction.

3. Scalar field in an external magnetic field

A free, real, scalar field $\phi(\mathbf{x},t)$ is described by the partition function

$$Z(\beta) = \int \mathscr{D}\phi \exp - \int_0^\beta \mathrm{d}\tau \int \mathrm{d}^3\mathbf{x} \left[\frac{1}{2}(\partial_\tau \phi)^2 + \frac{1}{2}(\nabla\phi)^2 + \frac{1}{2}m^2\phi^2 \right], \tag{12}$$

where $\beta = 1/T$ is the inverse temperature. The corresponding free energy was derived in [1]. The result is

$$\mathscr{F} \equiv -\frac{1}{\beta V}\ln Z(\beta) = \int \frac{\mathrm{d}^3\mathbf{k}}{(2\pi)^3}\left[\frac{\omega_\mathbf{k}}{2} + \frac{1}{\beta}\ln\left(1 - \mathrm{e}^{-\beta\omega_\mathbf{k}}\right)\right], \tag{13}$$

where $\omega_\mathbf{k} = \sqrt{m^2 + \mathbf{k}^2}$. The first term in the integrand gives rise to the zero-point energy, which is divergent. After dimensional regularization using the $\overline{\mathrm{MS}}$ scheme, this takes the form

$$\mathscr{E} = \int \frac{\mathrm{d}^d\mathbf{k}}{(2\pi)^d}\frac{\omega_\mathbf{k}}{2} = -\frac{1}{64\pi^2}m^4\left[\frac{1}{\varepsilon} + \ln\left(\frac{\Lambda^2}{m^2}\right) + \frac{3}{2}\right] + \mathscr{O}(\varepsilon), \tag{14}$$

in $d = 3 - 2\varepsilon$ dimensions, with Λ a mass scale introduced to ensure that $\mathscr{E}$ has the correct dimension. We will begin by generalizing this result to that of a complex scalar field in the presence of a constant external magnetic field. We define

$$\phi(x) = \frac{1}{\sqrt{2}}[\phi_1(x) + i\phi_2(x)], \tag{15}$$

$$\phi^*(x) = \frac{1}{\sqrt{2}}[\phi_1(x) - i\phi_2(x)], \tag{16}$$

where ϕ_1, ϕ_2 are real scalar fields, and introduce the Minkowskian Lagrangian density

$$\mathscr{L} = (\partial^\mu\phi)^*\,\partial_\mu\phi - m^2\phi^*\phi. \tag{17}$$

The Lagrangian has a global $U(1)$ symmetry, as it is invariant under the transformation

$$\phi \to \mathrm{e}^{i\alpha}\phi, \tag{18}$$

with α an arbitrary phase. The associated Noether-conserved current is

$$j^\mu = i\left(\phi\partial^\mu\phi^* - \phi^*\partial^\mu\phi\right).$$

To allow for a finite particle density, we must replace the canonical partition function with the grand canonical one. This is done by letting $\mathscr{H} \to \mathscr{H} - \mu j^0$, where $\mathscr{H}$ is the Hamiltonian density, related to the Lagrangian density by the Legendre transform

$$\mathscr{H} = \pi\phi + \pi^*\phi^* - \mathscr{L},$$

where

$$\pi = \frac{\partial \mathscr{L}}{\partial (\partial_0 \phi)} = \partial_0 \phi^*,$$
$$\pi^* = \frac{\partial \mathscr{L}}{\partial (\partial_0 \phi^*)} = \partial_0 \phi$$

are the canonical momenta. This gives

$$\begin{aligned}\mathscr{H} &= \pi^*\pi + \nabla\phi^*\nabla\phi + m^2\phi^*\phi \to \mathscr{H} - \mu j_0 \\ &= \pi^*\pi + \nabla\phi^*\nabla\phi + m^2\phi^*\phi - \mu i(\pi\phi - \pi^*\phi^*)\end{aligned}$$

We then perform the inverse Legendre transform to get the new Lagrangian:

$$\mathscr{L} = \pi^* \frac{\partial \mathscr{H}}{\partial \pi^*} + \pi \frac{\partial \mathscr{H}}{\partial \pi} - \mathscr{H} = \pi^* \partial_0 \phi^* + \pi \partial_0 \phi - \mathscr{H}.$$

The result is

$$\mathscr{L} \to (\partial_0 + i\mu)\phi^*(\partial_0 - i\mu)\phi - \nabla\phi^*\nabla\phi - m^2\phi^*\phi.$$

The corresponding Euclidean Lagrangian density is

$$\mathscr{L}_E = (\partial_0 + \mu)\phi^*(\partial_0 - \mu)\phi + \nabla\phi^*\nabla\phi + m^2\phi^*\phi.$$

The global $U(1)$ symmetry can be promoted to a local one , i.e., $\alpha \to \alpha(x)$, by the substitution

$$\partial_\mu \to D_\mu = \partial_\mu + iqA_\mu, \tag{19}$$

in the Lagrangian. Here, q is a dimensionless coupling constant, and A_μ is a four-vector field transforming as

$$A_\mu \to A_\mu - \frac{1}{q}\partial_\mu \alpha. \tag{20}$$

A gauge invariant kinetic term for the gauge field is of the form

$$\mathscr{L}_{\text{Maxwell}} = \frac{1}{4}F_{\mu\nu}F_{\mu\nu} = \frac{1}{4}(\partial_\nu A_\mu - \partial_\mu A_\nu)(\partial_\nu A_\mu - \partial_\mu A_\nu), \tag{21}$$

i.e. the Lagrangian of a free electromagnetic field. We will consider a constant, homogeneous magnetic field, neglecting quantum fluctuations. The vector potential

$$A = Bx\hat{y} \tag{22}$$

corresponds to a uniform magnetic field $\mathbf{B} = B\hat{z}$ pointing in the $\hat{z}$ direction. This choice of vector potential is known as the Landau gauge; an equivalent, commonly seen choice is $A = \frac{1}{2}B(x\hat{y} - y\hat{x})$, known as the symmetric gauge.

The Euclidean action is then

$$S_E = \int_0^\beta \mathrm{d}\tau \int \mathrm{d}^3\mathbf{x} \left[(\partial_\tau + \mu)\phi^*(\partial_\tau - \mu)\phi + \partial_x\phi^*\partial_x\phi + (\partial_y - iqBx)\phi^*(\partial_y + iqBx)\phi + \partial_z\phi^*\partial_z\phi + m^2\phi^*\phi\right] + \frac{\beta V}{2}B^2 \tag{23}$$

After integration by parts, this becomes

$$S_E = -\int_0^\beta \mathrm{d}\tau \int \mathrm{d}^3\mathbf{x}\phi^* \left[(\partial_\tau - \mu)^2 + \partial_x^2 + (\partial_y + iqBx)^2 + \partial_z^2 - m^2\right]\phi + \frac{\beta V}{2}B^2 \tag{24}$$

$$\equiv \int_0^\beta \mathrm{d}\tau \int \mathrm{d}^3\mathbf{x}\phi^* D\phi + \frac{\beta V}{2}B^2 \tag{25}$$

As in [1], we will solve the functional integral

$$Z = \int \mathscr{D}\phi^* \mathscr{D}\phi \mathrm{e}^{-S_E} \tag{26}$$

by diagonalizing the operator D. The eigenvalue equation

$$D\phi = E\phi \tag{27}$$

can be solved by separation of variables, and so we write

$$\phi = T(\tau)X(x)Y(y)Z(z) \tag{28}$$

The solution is

$$T(\tau) = \mathrm{e}^{i\omega_n\tau}, \tag{29}$$

$$Y(y) = \mathrm{e}^{ip_y y}, \tag{30}$$

$$Z(z) = \mathrm{e}^{ip_z z}, \tag{31}$$

$$\tag{32}$$

with $X(x)$ a solution of

$$-\left[\frac{\mathrm{d}^2}{\mathrm{d}x^2} - (p_y + qBx)^2\right]X(x) = \left[E - (\omega_n + i\mu)^2 - p_z^2 - m^2\right]X(x). \tag{33}$$

With $x' = x - x_0 = x + \frac{p_y}{qB}$, $\omega_c = |qB|$, and $E' = E - (\omega_n + i\mu)^2 - p_z^2 - m^2$, this becomes

$$\left(-\frac{\mathrm{d}^2}{\mathrm{d}x'^2} + \omega_c^2 x'^2\right)X(x') = E'X(x'), \tag{34}$$

which can be recognized as the well-known Schrödinger equation for a one dimensional harmonic oscillator. A complete and orthonormal set of solutions $X_l(x')$ exists, where l is any non-negative integer and the corresponding eigenvalue is $E'_l = (2l+1)\,\omega_c$. A general linear combination of solutions is of the form

$$\phi(\tau,x,y,z) = \frac{1}{L\sqrt{\beta}} \sum_{n=-\infty}^{\infty} \sum_{l=0}^{\infty} \sum_{p_y,p_z} \phi_{n,m}(p_y,p_z)\mathrm{e}^{i(\omega_n\tau + p_y y + p_z z)} X_l(x + \tfrac{p_y}{qB}), \tag{35}$$

where $\omega_n = \frac{2\pi n}{\beta}$ are the bosonic Matsubara frequencies. With periodic boundary conditions and a cubic integration volume of linear dimension L, p_z takes all values of the form $p_z = \frac{2\pi k}{L}$ with k integer. p_y takes

values of the same form, but since x_0 must lie within the boundaries of the system, p_y is subject to the constraint $|\frac{p_y}{qB}| < \frac{L}{2}$. The corresponding action is

$$S_E = \int_0^\beta \int_V \mathrm{d}^3\mathbf{x} \frac{1}{\beta L^2} \sum_{n,l,p_y,p_z} \sum_{u,v,q_y,q_z} \phi^*_{u,v,q_y,q_z} \phi_{n,l,p_y,p_z} E(\mu, p_z, \omega_n, m)$$
$$\times \exp\{i[(\omega_n - \omega_u)\tau + (p_y - q_y)y + (p_z - q_z)z]\} X_l\left(x + \frac{p_y}{qB}\right) X_v\left(x + \frac{k_y}{qB}\right), \tag{36}$$

The integrals over τ, y and z produce a factor of $\beta L^2 \delta_{n,u}\delta_{p_y,k_y}\delta_{p_z,k_z}$. The remaining integral over x approaches $\delta_{l,y}$ as $L \to \infty$. We get

$$S_E = \sum_{n,l,p_y,p_z} |\phi_{n,l,p_y,p_z}|^2 E(\mu, \omega_n, l, p_z). \tag{37}$$

We can write the partition function as

$$Z = \prod_{l,n,p_y,p_z} \int \mathrm{d}\phi_{l,n,p_y,p_z} \exp\left[-\sum_{n,l,p_y,p_z} |\phi_{n,l,p_y,p_z}|^2 E(\mu, \omega_n, l, p_z)\right], \tag{38}$$

which is just a product of Gaussian integrals. Up to a constant, we have

$$-\ln Z = \sum_{l,n,p_y,p_z} \ln\left[E(\mu, l, n, p_z)\right] = \sum_{l,n,p_y,p_z} \ln\left[(\omega_n + i\mu)^2 + p_z^2 + M_B^2\right], \tag{39}$$

where $M_B^2 = m^2 + (2l+1)|qB|$. The sum over p_y gives a factor of $\frac{|qB|L^2}{2\pi}$. The sum over ω_n is calculated in Appendix A.1. Using Eq. (A.41), we get

$$-\ln Z = \frac{|qB|L^2}{2\pi} \sum_{l,p_z} \left[\beta\sqrt{p_z^2 + M_B^2} + \ln\left(1 - \mathrm{e}^{-\beta\left(\sqrt{p_z^2+M_B^2} - \mu\right)}\right) + \ln\left(1 - \mathrm{e}^{-\beta\left(\sqrt{p_z^2+M_B^2} + \mu\right)}\right)\right], \tag{40}$$

where we have discarded the integration constant of Eq (A.41), since it is independent on $\omega_{\mathbf{k}}$ and on β. When $L \to \infty$, the sum over p_z becomes an integral,

$$\sum_{p_z} = \frac{1}{\Delta p_z} \sum_{p_z} \Delta p_z \to \frac{1}{\Delta p_z} \int \mathrm{d}p_z, \tag{41}$$

where $\Delta p_z = 2\pi/L$. We then have

$$\mathscr{F} = -\frac{1}{\beta V} \ln Z = \frac{|qB|}{2\pi} \sum_l \int \frac{\mathrm{d}p_z}{2\pi} \left[\sqrt{p_z^2 + M_B^2} + \frac{1}{\beta}\ln\left(1 - \mathrm{e}^{-\beta\left(\sqrt{p_z^2+M_B^2} - \mu\right)}\right) + \frac{1}{\beta}\ln\left(1 - \mathrm{e}^{-\beta\left(\sqrt{p_z^2+M_B^2} + \mu\right)}\right)\right]. \tag{42}$$

The vacuum term in (42) is divergent, and we perform the integral over p_z using dimensional regularization in Appendix A. Using Eq. (A.10), we have

$$\mathscr{E} = \frac{|qB|}{2\pi} \sum_l \int \frac{\mathrm{d}p_z}{2\pi} \sqrt{p_z^2 + M_B^2} \to \frac{|qB|}{2\pi} \sum_l -\frac{M_B^2}{4\pi}\left(\frac{4\pi\Lambda^2}{M_B^2}\right)^\varepsilon \Gamma(-1+\varepsilon) + \mathscr{O}(\varepsilon) \tag{43}$$

After substituting

$$M_B^2 = 2|qB|\left(l+\frac{1}{2}+\frac{m^2}{2|qB|}\right) = 2|qB|\left(l+\frac{1}{2}+x\right), \tag{44}$$

we get

$$\mathscr{E} = -\frac{(qB)^2}{4\pi^2}\left(\frac{2\pi\Lambda^2}{|qB|}\right)^{\varepsilon}\Gamma(-1+\varepsilon)\sum_l\left(l+\frac{1}{2}+x\right)^{1-\varepsilon}. \tag{45}$$

The sum is divergent for $\mathrm{Re}(\varepsilon) < 2$, but can be analytically continued to all $\varepsilon \neq 2$. The Hurwitz zeta function $\zeta(s,a)$ is defined as the analytic continuation of

$$\sum_{l=0}^{\infty}\frac{1}{(l+a)^s} \tag{46}$$

to all $s \neq 1$. We regularize the sum in (45) by replacing it with this function, i.e.

$$\mathscr{E} \to -\frac{(qB)^2}{4\pi^2}\left(\frac{2\pi\Lambda^2}{|qB|}\right)^{\varepsilon}\Gamma(-1+\varepsilon)\zeta(-1+\varepsilon,\tfrac{1}{2}+x). \tag{47}$$

Expanding in ε, we have

$$\left(\frac{2\pi\Lambda^2}{|qB|}\right)^{\varepsilon} = 1+\varepsilon\ln\left(\frac{2\pi\Lambda^2}{|qB|}\right)+\mathscr{O}(\varepsilon^2), \tag{48}$$

$$\Gamma(-1+\varepsilon) = -\frac{1}{\varepsilon}+\gamma_E-1+\mathscr{O}(\varepsilon), \tag{49}$$

$$\zeta(-1+\varepsilon,\tfrac{1}{2}+x) = \zeta(-1,\tfrac{1}{2}+x)+\varepsilon\zeta^{(1,0)}(-1,\tfrac{1}{2}+x)+\mathscr{O}(\varepsilon^2), \tag{50}$$

where $\zeta(-1,\frac{1}{2}+x) = \frac{1}{24}-\frac{1}{2}x^2$ and $\zeta^{(1,0)}$ indicates differentiation with respect to the first argument. After the substitution $\Lambda^2 \to \frac{e^{\gamma_E}}{4\pi}\Lambda^2$, this reduces to

$$\mathscr{E} = \frac{1}{32\pi^2}\left\{\left[\frac{1}{\varepsilon}+\ln\frac{\Lambda^2}{2|qB|}+1\right]\left[\frac{(qB)^2}{3}-m^4\right]+8(qB)^2\zeta^{(1,0)}(-1,\frac{1}{2}+x)\right\}+\mathscr{O}(\varepsilon) \tag{51}$$

4. Fermions in an external magnetic field

For fermions in an external magnetic field, the eigenvalue spectrum of the Dirac operator is

$$E(\omega_n,l,s,p_z) = (\omega_n+i\mu)^2+p_z^2+m^2+(2l+1-s)|q_fB|. \tag{52}$$

The derivation is analogous to the bosonic case. Here, ω_n are the fermionic Matsubara frequencies, $s=\pm1$ is the spin, and q_f is the charge of the fermion. We have

$$-\ln Z = -\frac{|q_fB|V}{2\pi}\sum_{n,l,s}\int\frac{\mathrm{d}p_z}{2\pi}\ln\left[(\omega_n+i\mu)^2+p_z^2+M_f^2\right], \tag{53}$$

where $M_f^2 = m^2 + (2l+1-s)|qB|$. Using (A.37), we get

$$\mathscr{F} = -\frac{|q_f B|}{2\pi}\sum_{l,s}\int\frac{\mathrm{d}p_z}{2\pi}\left\{\sqrt{p_z^2+M_f^2}+\frac{1}{\beta}\ln\left[1+\mathrm{e}^{-\beta\left(\sqrt{p_z^2+M_f^2}+\mu\right)}\right]+\frac{1}{\beta}\ln\left[1+\mathrm{e}^{-\beta\left(\sqrt{p_z^2+M_f^2}-\mu\right)}\right]\right\}. \tag{54}$$

The vacuum energy density is

$$\mathscr{E} = -\frac{|q_f B|}{2\pi}\sum_{l,s}\int\frac{\mathrm{d}p_z}{2\pi}\sqrt{p_z^2+M_f^2}. \tag{55}$$

This has the same form as Eq. (43), and we get

$$\mathscr{E} = \frac{(qB)^2}{4\pi^2}\left(\frac{2\pi\Lambda^2}{|qB|}\right)^{\varepsilon}\Gamma(-1+\varepsilon)\sum_{l,s}\left(l+\frac{1-s}{2}+x\right)^{1-\varepsilon}, \tag{56}$$

$$\tag{57}$$

The sum in (56) can be written as

$$\sum_{l,s}\left(l+\frac{1-s}{2}+x\right)^{1-\varepsilon} = \sum_l (l+x)^{1-\varepsilon}+\sum_l (1+l+x)^{1-\varepsilon} = 2\sum_l (l+x)^{1-\varepsilon} - x^{1-\varepsilon} \tag{58}$$

$$\tag{59}$$

As before, this is regularized using the Hurwitz zeta function:

$$\sum_l (l+x)^{1-\varepsilon} \to \zeta(-1+\varepsilon,x). \tag{60}$$

Expanding in powers of ε, we have

$$2\zeta(-1+\varepsilon,x) - x^{1-\varepsilon} = 2\zeta(-1,x) + 2\varepsilon\zeta^{(1,0)}(-1,x) - x(1-\varepsilon\ln x) + \mathscr{O}(\varepsilon^2), \tag{61}$$

$$\to 2\zeta(-1+\varepsilon,x) - x^{1-\varepsilon} = -\frac{1}{6} - x^2 + x + 2\varepsilon\zeta^{(1,0)}(-1,x) - x(1-\varepsilon\ln x) + \mathscr{O}(\varepsilon^2). \tag{62}$$

We then have

$$\begin{aligned}\mathscr{E} &= \frac{(q_f B)^2}{4\pi^2}\left[1+\varepsilon\ln\frac{\Lambda^2}{2|q_f B|}\right]\left[\frac{1}{\varepsilon}+1\right]\left[-\frac{1}{6}-x^2+2\varepsilon\zeta^{(1,0)}(-1,x)+\varepsilon x\ln x\right]+\mathscr{O}(\varepsilon)\\ &= \frac{1}{16\pi^2}\left\{\left(\frac{1}{\varepsilon}+\ln\frac{\Lambda^2}{2|q_f B|}+1\right)\left[\frac{2(q_f B)^2}{3}+m^4\right]-8(q_f B)^2\zeta^{(1,0)}(-1,x)-2|q_f B|m^2\ln x\right\}+\mathscr{O}(\varepsilon).\end{aligned} \tag{63}$$

5. Quark-Meson Model

In this section we will use the results we have obtained so far to study the quark-meson (QM) model (also known as the linear sigma model coupled to quarks, or $\mathrm{LSM_q}$). It was originally proposed by Yukawa [16] as a model of the interactions between nucleons through exchange of pions. In later years,

this model has also been used as an effective model of QCD at low energies. By construction, it has an $SU(2) \times SU(2) \times U(1)$ symmetry which is broken down to $SU(2) \times U(1)$in the vacuum, as is the case in two-flavor QCD. Therefore, it can be used to model the chiral phase transition of QCD, i.e. the transition between phases of broken and unbroken chiral symmetry. The model includes the quarks as massless fermions coupled to a four-component scalar field. In this model, the quarks are not confined, but there exists an extension of the model, the Polyakov-quark-meson model, which incorporates quark confinement [17].

The Euclidean Lagrangian density is given by

$$\mathscr{L}_E = \mathscr{L}_{\text{meson}} + \mathscr{L}_{\text{quark}} + \mathscr{L}_{\text{Yukawa}}, \tag{64}$$

where

$$\mathscr{L}_{\text{meson}} = \frac{1}{2}\partial_\mu \phi_i \partial_\mu \phi_i + \frac{1}{2}m^2 \phi_i \phi_i + \frac{1}{4!}\lambda(\phi_i \phi_i)^2 - h\sigma, \tag{65}$$

$$\mathscr{L}_{\text{quark}} = \bar{\psi}(\partial\!\!\!/ - \mu\gamma_0)\psi, \tag{66}$$

$$\mathscr{L}_{\text{Yukawa}} = g\bar{\psi}(\sigma + i\gamma_5 \vec{\tau}\cdot\vec{\pi})\psi, \tag{67}$$

where $i = 1,2,3,4$, and

$$(\phi_1, \phi_2, \phi_3, \phi_4) = (\sigma, \pi_0, \pi_1, \pi_2) = (\sigma, \vec{\pi}). \tag{68}$$

$$\psi = \begin{pmatrix} u \\ d \end{pmatrix} \tag{69}$$

is an isospin doublet, with u and d the up and down quarks (in Yukawa's model, the proton and neutron), with no bare mass. $\mu = \text{diag}(\mu_u, \mu_d)$ is the quark chemical potential. $\vec{\tau} = (\tau_1, \tau_2, \tau_3)$ are the Pauli matrices, acting on the isospin indices of ψ.

The quark sector of the Lagrangian is invariant under $U(2)$ transformations, which decompose into $SU(2) \times U(1)$, in isospin space. Without a quark mass term, the left- and right-chiral components decouple, and $\mathscr{L}_{\text{quark}}$ becomes invariant under $U(2)_L \times U(2)_R \sim SU(2)_L \times SU(2)_R \times U(1)_V \times U(1)_A$. In addition, the quark fields belong to the fundamental representation of the group $SU(N_c)$, where N_c is the number of colors. while in QCD this symmetry is a local one, we leave it as a global symmetry in this model.

$\mathscr{L}_{\text{meson}}$ alone is known as the $O(4)$ linear sigma model. Note that when $h = 0$ this Lagrangian is invariant under $O(4)$ transformations. When m^2 is negative, this symmetry is broken in the vacuum, which only respects $O(3)$ symmetry. When $h \neq 0$ the symmetry is explicitly broken in the Lagrangian. $O(4)$ is locally isomorphic to $SU(2) \times SU(2)$. For $U, V \in SU(2)$ the transformation

$$\sigma + i\vec{\pi}\cdot\vec{\tau} \to V(\sigma + i\vec{\pi}\cdot\vec{\tau})U^{-1} = \sigma' + i\vec{\pi}'\cdot\vec{\tau} \tag{70}$$

leaves $\mathscr{L}_{\text{meson}}$ invariant, since

$$\sigma'^2 + \vec{\pi}'^2 \propto \det(\sigma' + i\vec{\pi}'\cdot\vec{\tau}) = \det(V)\det(\sigma + i\vec{\pi}\cdot\vec{\tau})\det(U^{-1}) = \det(\sigma + i\vec{\pi}\cdot\vec{\tau}) \tag{71}$$

with $\sigma', \vec{\pi}'$ real given real $\sigma, \vec{\pi}$ [1]. In terms of the chiral fields, the interaction term is

$$\mathscr{L}_{\text{Yukawa}} = g\bar{\psi}_L(\sigma - i\gamma_5\vec{\tau}\cdot\vec{\pi})\psi_R + g\bar{\psi}_R(\sigma + i\gamma_5\vec{\tau}\cdot\vec{\pi})\psi_L \tag{72}$$

[1] This follows from the fact that any 2×2 unitary matrix can be written $U = aI + \vec{b}\cdot\vec{\tau}$ with $a, \vec{b}$ real, and the fact that the product of two unitary matrices is unitary.

Clearly, the transformation

$$\begin{aligned} \psi_R &\to U\psi_R, \\ \psi_L &\to V\psi_L, \\ \sigma + i\vec{\pi}\cdot\vec{\tau} &\to V(\sigma + i\vec{\pi}\cdot\vec{\tau})U^{-1} \end{aligned} \tag{73}$$

leaves the full Lagrangian invariant when $h = 0$. We can also make $U(1)_V$ transformations, however the $U(1)_A$ symmetry is not respected by the interaction term. Thus the symmetry group of the full Lagrangian with $h = 0$ is $SU(2)_L \times SU(2)_R \times U(1)_V$.

In general, the expectation value of the four-component scalar field can point in any direction in ϕ-space. However, by making the appropriate transformation (70), we can always ensure that it points in the σ direction. Thus, without loss of generality, we can set

$$\sigma = \phi_0 + \tilde{\sigma}, \tag{74}$$

such that

$$\langle\tilde{\sigma}\rangle = \langle\vec{\pi}\rangle = 0. \tag{75}$$

The expectation value of the σ field in this model corresponds to the chiral condensate $\langle\bar{\psi}\psi\rangle$ of QCD [18]. In the one-loop approximation, we keep only the terms quadratic in the quantum fields in the Lagrangian density. This leaves us with

$$\begin{aligned} \mathscr{L}_{\text{meson}} &\approx \frac{1}{2}m^2\phi_0^2 + \frac{1}{4!}\lambda\phi_0^4 - h\phi_0 + \frac{1}{2}\partial_\mu\tilde{\sigma}\partial_\mu\tilde{\sigma} + \frac{1}{2}\left(m^2 + \frac{1}{2}\lambda\phi_0^2\right)\tilde{\sigma}^2 + \frac{1}{2}\partial_\mu\vec{\pi}\partial_\mu\vec{\pi} + \frac{1}{2}\left(m^2 + \frac{1}{6}\lambda\phi_0^2\right)\vec{\pi}^2 \\ &\equiv V(\phi_0) + \frac{1}{2}\partial_\mu\tilde{\sigma}\partial_\mu\tilde{\sigma} + \frac{1}{2}m_\sigma^2\tilde{\sigma}^2 + \frac{1}{2}\partial_\mu\vec{\pi}\partial_\mu\vec{\pi} + \frac{1}{2}m_\pi^2\vec{\pi}^2, \end{aligned} \tag{76}$$

and

$$\mathscr{L}_{\text{Yukawa}} \approx g\bar{\psi}\phi_0\psi, \tag{77}$$

so that

$$\begin{aligned} \mathscr{L}_{\text{quark}} + \mathscr{L}_{\text{Yukawa}} &\approx \bar{\psi}(\gamma_\mu\partial_\mu - \mu\gamma_0 + g\phi_0)\psi \\ &= \bar{\psi}(\gamma_\mu\partial_\mu - \mu\gamma_0 + m_q)\psi. \end{aligned} \tag{78}$$

When $\phi_0 \neq 0$, the quarks acquire an effective mass $m_q = g\phi_0$, which mixes the left and right chiral components and leads to the breaking of chiral symmetry. That is, $SU(2)_L \times SU(2)_R \times U(1)_V$ is broken down to $SU(2) \times U(1)_V$. Note that if $h = 0$, then in the vacuum, we have $\langle\sigma\rangle = \sqrt{-6m^2}$, which is the minimum of the tree-level potential. Thus the pion mass $m_\pi^2 = m^2 + \frac{1}{6}\phi_0^2$ is zero. Since $SU(2)$ has three generators, and there are three pions, this is in accordance with Goldstone's theorem.

In order to incorporate a magnetic field, we define the charged pion fields

$$\pi_\pm = \frac{1}{\sqrt{2}}(\pi_1 \pm i\pi_2). \tag{79}$$

The meson sector of the QM Lagrangian then takes the form

$$\mathscr{L}_{\text{meson}} = \frac{1}{2}\partial_\mu\sigma\partial_\mu\sigma + \frac{1}{2}\partial_\mu\pi_0\partial_\mu\pi_0 + \partial_\mu\pi_-\partial_\mu\pi_+ + \frac{1}{2}m^2\left(\sigma^2 + \pi_0^2 + 2\pi_-\pi_+\right) + \frac{1}{4!}\lambda\left(\sigma^2 + \pi_0^2 + 2\pi_-\pi_+\right)^2 - h\sigma. \tag{80}$$

The charged pions are then coupled to an electromagnetic field via a covariant derivative

$$\partial_\mu \pi_- \partial_\mu \pi_+ \to D^*_\mu \pi_- D_\mu \pi_+ = (\partial_\mu - iqA_\mu)\pi_-(\partial_\mu + iqA_\mu)\pi_+. \tag{81}$$

Similarly, we let

$$\mathscr{L}_{\text{quark}} \to \sum_f \bar{\psi}_f(\partial\!\!\!/ + iq_f A\!\!\!/ - \mu_f \gamma_0)\psi_f, \tag{82}$$

and add the kinetic term for the EM field,

$$\mathscr{L}_{\text{Maxwell}} = \frac{1}{4}F_{\mu\nu}F_{\mu\nu}. \tag{83}$$

In a constant magnetic field as given by (22), we simply have

$$\mathscr{L}_{\text{Maxwell}} = \frac{1}{2}B^2. \tag{84}$$

The tree level potential is

$$V_0(\phi_0, B) = \frac{1}{2}m^2\phi_0^2 + \frac{\lambda}{4!}\phi_0^4 - h\phi_0 + \frac{1}{2}B^2. \tag{85}$$

Using the results from the previous sections, we can now write down the effective potential

$$V_{\text{eff}}(\phi_0) = -\frac{1}{\beta V}\ln Z \tag{86}$$

to one-loop order. The contributions from the electrically neutral $\tilde{\sigma}$ and π_0 fields are given by Eqs. (13) and (14),

$$V^{\sigma}_{\text{eff}} = -\frac{1}{64\pi^2}m_\sigma^4\left[\frac{1}{\varepsilon} + \ln\left(\frac{\Lambda^2}{m_\sigma^2}\right) + \frac{3}{2}\right] + \frac{1}{\beta}\int\frac{\mathrm{d}^3\mathbf{k}}{(2\pi)^3}\left[\ln\left(1 - \mathrm{e}^{-\beta\omega_\sigma(\mathbf{k})}\right)\right], \tag{87}$$

$$V^{\pi_0}_{\text{eff}} = -\frac{1}{64\pi^2}m_\pi^4\left[\frac{1}{\varepsilon} + \ln\left(\frac{\Lambda^2}{m_\pi^2}\right) + \frac{3}{2}\right] + \frac{1}{\beta}\int\frac{\mathrm{d}^3\mathbf{k}}{(2\pi)^3}\left[\ln\left(1 - \mathrm{e}^{-\beta\omega_\pi(\mathbf{k})}\right)\right], \tag{88}$$

where $\omega_{\sigma,\pi}(\mathbf{k}) = \sqrt{\mathbf{k}^2 + m^2_{\sigma,\pi}}$. The contribution from the charged pions is given by equations (42) and (51):

$$V^{\pi^\pm}_{\text{eff}} = \frac{1}{32\pi^2}\left\{\left[\frac{1}{\varepsilon} + \ln\frac{\Lambda^2}{2|eB|} + 1\right]\left[\frac{(eB)^2}{3} - m_\pi^4\right] + 8(eB)^2\zeta^{(1,0)}(-1, \frac{1}{2} + x)\right\} \tag{89}$$

$$+ \frac{|eB|}{2\pi\beta}\sum_l\int\frac{\mathrm{d}p_z}{2\pi}\left[\ln\left(1 - \mathrm{e}^{-\beta\left(\sqrt{p_z^2 + M_B^2} - \mu_\pi\right)}\right) + \ln\left(1 - \mathrm{e}^{-\beta\left(\sqrt{p_z^2 + M_B^2} + \mu_\pi\right)}\right)\right], \tag{90}$$

where $\pm e$ is the charge of the pions (equal in magnitude to the electron charge), $x = \frac{m_\pi^2}{2|qB|}$ and $M_B^2 = m_\pi^2 + (2l+1)|eB|$. The contribution from the quarks is given by Eqs. (54) and (63):

$$V^{\text{q}}_{\text{eff}} = \sum_{f=u,d}\frac{1}{16\pi^2}\left\{\left(\frac{1}{\varepsilon} + \ln\frac{\Lambda^2}{2|q_fB|} + 1\right)\left[\frac{2(q_fB)^2}{3} + m_q^4\right] - 8(q_fB)^2\zeta^{(1,0)}(-1, x_f) - 2|q_fB|m_q^2\ln x_f\right\} \tag{91}$$

$$- \sum_{f=u,d}\frac{|q_fB|}{2\beta\pi}\sum_{f,l,s}\int\frac{\mathrm{d}p_z}{2\pi}\left\{\ln\left[1 + \mathrm{e}^{-\beta\left(\sqrt{p_z^2 + M_f^2} - \mu_f\right)}\right] + \ln\left[1 + \mathrm{e}^{-\beta\left(\sqrt{p_z^2 + M_f^2} + \mu_f\right)}\right]\right\}, \tag{92}$$

where $q_u = \frac{2}{3}|e|$, $q_d = -\frac{1}{3}|e|$, $x_f = \frac{m_q^2}{2|q_f B|}$ The divergent terms are

$$V_{\rm eff}^{\rm div} = \frac{1}{64\pi^2\varepsilon}\left[\frac{2(eB)^2}{3} - 3m_\pi^2 - m_\sigma^2 + N_c\sum_f\left(\frac{8(q_f B)^2}{3} + 4m_q^2\right)\right]. \tag{93}$$

To eliminate these divergences we first renormalize A_μ such that

$$B^2 \to B^2\left[1 - \frac{q^2}{48\pi^2\varepsilon} - N_c\sum_f\frac{q_f^2}{12\pi^2\varepsilon}\right], \tag{94}$$

Using the tree-level relations between the field-dependent masses and the parameters of the model (Eqs. (76)-(78)), the remaining divergences can be written

$$V_{\rm eff}^{\rm div} = -\frac{1}{64\pi^2\varepsilon}m_\sigma^4 - \frac{3}{64\pi^2\varepsilon}m_\pi^4 + \frac{N_c}{8\pi^2\varepsilon}m_q^4 \tag{95}$$

$$= -\frac{m^4}{16\pi^2\varepsilon} - \frac{\lambda m^2}{32\pi^2\varepsilon}\phi_0^2 + \left[-\frac{\lambda^2}{192\pi^2\varepsilon} + \frac{N_c g^4}{8\pi^2\varepsilon}\right]\phi_0^4 \tag{96}$$

These are eliminated by renormalizing the vacuum energy, meson masses and the coupling constant,

$$\mathscr{E} \to \mathscr{E} + \delta\mathscr{E}, \tag{97}$$

$$m^2 \to m^2 + \delta m^2, \tag{98}$$

$$\lambda \to \lambda + \delta\lambda, \tag{99}$$

with the counterterms

$$\delta\mathscr{E} = \frac{m^4}{16\pi^2\varepsilon}, \tag{100}$$

$$\delta m^2 = \frac{\lambda m^2}{16\pi^2\varepsilon}, \tag{101}$$

$$\delta\lambda = \frac{\lambda^2}{8\pi^2\varepsilon} - \frac{3N_c g^4}{2\pi^2\varepsilon}. \tag{102}$$

The vacuum part of the potential then becomes

$$\begin{aligned} V_{\rm eff}^{\rm vac} = {} & \frac{1}{2}m^2\phi_0^2 + \frac{\lambda}{4!}\phi_0^4 - h\phi_0 + \frac{1}{2}B^2 - \frac{1}{64\pi^2}m_\sigma^4\left[\ln\left(\frac{\Lambda^2}{m_\sigma^2}\right) + \frac{3}{2}\right] - \frac{1}{64\pi^2}m_\pi^4\left[\ln\left(\frac{\Lambda^2}{m_\pi^2}\right) + \frac{3}{2}\right] \\ & + \frac{1}{64\pi^2}\left\{\left[\ln\frac{\Lambda^2}{2|qB|} + 1\right]\left[\frac{(qB)^2}{3} - m_\pi^4\right] + 8(qB)^2\zeta^{(1,0)}(-1, \frac{1}{2} + x)\right\} \\ & + \sum_f\frac{N_c}{16\pi^2}\left\{\left(\ln\frac{\Lambda^2}{2|q_f B|} + 1\right)\left[\frac{2(q_f B)^2}{3} + m_q^4\right] - 8(q_f B)^2\zeta^{(1,0)}(-1, x_f) - 2|q_f B|m_q^2\ln x_f\right\}. \end{aligned} \tag{103}$$

The thermal part is

$$\begin{aligned} V_{\rm eff}^{\rm thermal} = {} & \frac{1}{\beta}\int\frac{{\rm d}^3\mathbf{k}}{(2\pi)^3}\Big(\ln\{1 - \exp[-\beta\omega_\sigma(\mathbf{k})]\} + \ln\{1 - \exp[-\beta\omega_\pi(\mathbf{k})]\}\Big) \\ & + \frac{|qB|}{\pi\beta}\sum_l\int\frac{{\rm d}p_z}{2\pi}\ln\left(1 - {\rm e}^{-\beta\sqrt{p_z^2 + M_\pi^2}}\right) \\ & - \frac{N_c}{2\beta\pi}\sum_{f,l,s}|q_f B|\int\frac{{\rm d}p_z}{2\pi}\left\{\ln\left[1 + {\rm e}^{-\beta\left(\sqrt{p_z^2 + M_f^2} - \mu\right)}\right] + \ln\left[1 + {\rm e}^{-\beta\left(\sqrt{p_z^2 + M_f^2} + \mu\right)}\right]\right\}, \end{aligned} \tag{104}$$

with $M_\pi = \sqrt{m_\pi^2 + (2l+1)|qB|}$, $M_f = \sqrt{m_q^2 + (2l+1-s)|q_f B|}$. The sum over l and s in the last term can be rewritten using

$$\sum_{l=0}^{\infty}\sum_{s=\pm 1} f(2l+1-s) = \sum_{l=0}^{\infty} f(2l) + \sum_{l=1}^{\infty} f(2l) = \sum_{l=0}^{\infty} \alpha_l f(2l), \tag{105}$$

with $\alpha_l = 2 - \delta_{l0}$. We will adopt the large-N_c approximation, which amounts to neglecting the vacuum and thermal fluctuations of the meson fields. In this approximation eqs. (103) and (104) reduce to

$$\begin{aligned} V_{\rm eff} = V_{\rm eff}^{\rm vac} + V_{\rm eff}^{\rm thermal} &= \frac{1}{2}m^2\phi_0^2 + \frac{\lambda}{4!}\phi_0^4 - h\phi_0 + \frac{1}{2}B^2 \\ &+ \frac{N_c}{16\pi^2}\sum_f \left\{ \left(\ln\frac{\Lambda^2}{2|q_f B|} + 1 \right) \left[\frac{2(q_f B)^2}{3} + m_q^4 \right] - 8(q_f B)^2 \zeta^{(1,0)}(-1, x_f) - 2|q_f B| m_q^2 \ln x_f \right\} \\ &- \frac{N_c}{2\beta\pi}\sum_{f,l} \alpha_l |q_f B| \int \frac{{\rm d}p_z}{2\pi} \left\{ \ln\left[1 + {\rm e}^{-\beta\left(\sqrt{p_z^2 + M_l^2} - \mu\right)} \right] + \ln\left[1 + {\rm e}^{-\beta\left(\sqrt{p_z^2 + M_l^2} + \mu\right)} \right] \right\}, \end{aligned} \tag{106}$$

where $M_l = \sqrt{m_q^2 + 2l|q_f B|}$. In the limit of small B, this expression is somewhat simplified. For large x, we have

$$\zeta^{(1,0)}(-1, x) \sim \frac{1}{2}x^2\left(\ln x - \frac{1}{2}\right) - \frac{1}{2}x\ln x. \tag{107}$$

Inserting this in (106), we get for the vacuum part of the potential:

$$\begin{aligned} V_{\rm eff}^{\rm vac} &\sim \frac{1}{2}m^2\phi_0^2 + \frac{\lambda}{4!}\phi_0^4 - h\phi_0 + \frac{1}{2}B^2 \\ &+ \frac{N_c}{16\pi^2}\sum_f \left\{ \left(\ln\frac{\Lambda^2}{2|q_f B|} + 1 \right) \left[\frac{2(q_f B)^2}{3} + m_q^4 \right] - 8(q_f B)^2 \left[\frac{1}{2}x_f^2\left(\ln x_f - \frac{1}{2} \right) - \frac{1}{2}x_f \ln x_f \right] - 2|q_f B| m_q^2 \ln x_f \right\}. \end{aligned} \tag{108}$$

After inserting $x_f = m_q^2/2|q_f B|$, this expression simplifies to

$$\begin{aligned} V_{\rm eff}^{\rm vac} &\sim \frac{1}{2}m^2\phi_0^2 + \frac{\lambda}{4!}\phi_0^4 - h\phi_0 + \frac{1}{2}B^2 \\ &+ \frac{N_c}{16\pi^2}\sum_f \left[m_q^4\left(\ln\frac{\Lambda^2}{m_q^2} + \frac{3}{2} \right) + \frac{2}{3}(q_f B)^2\left(\ln\frac{\Lambda^2}{2|q_f B|} + 1 \right) \right]. \end{aligned} \tag{109}$$

Furthermore, the sum over l can be approximated using the Euler-Maclaurin formula,

$$\sum_{n=a}^{b} f(n) \sim \int_a^b f(n){\rm d}n + \frac{1}{2}\left[f(a) + f(b) \right] + \sum_{k=1}^{\infty} \frac{B_{2k}}{(2k)!}\left[f^{(2k-1)}(b) - f^{(2k-1)}(a) \right], \tag{110}$$

where B_n are the Bernoulli numbers. The last term in (106) is of the form

$$S = 2\sum_{l=0}^{\infty} |q_f B| f\left[2l|q_f B| \right] - |q_f B| f(0) \sim 2|q_f B| \int_0^{\infty} {\rm d}l f(2|q_f B| l) + 2|q_f B| \sum_{k=1}^{\infty} \frac{B_{2k}}{(2k)!}\left[\frac{{\rm d}^{2k-1}}{{\rm d}l^{2k-1}} f(2|q_f B| l) \right]_{l=0}, \tag{111}$$

with

$$f(x) = -\frac{N_c}{2\pi\beta}\sum_f \int \frac{\mathrm{d}p_z}{2\pi} \ln\left[1+\mathrm{e}^{-\beta\left(\sqrt{p_z^2+m_q^2}+x\pm\mu\right)}\right]. \tag{112}$$

After defining $p_\perp^2 = 2|q_f B|l$, this can be rewritten as

$$S \sim \int_0^\infty 2p_\perp \mathrm{d}p_\perp f(p_\perp^2) + \sum_{k=1}^\infty \frac{B_{2k}}{(2k)!}(2|q_f B|)^{2k} f^{(2k-1)}(0) \tag{113}$$

Inserting this in (106), using

$$f'(0) = \frac{N_c}{4\pi}\sum_f \int \frac{\mathrm{d}p_z}{2\pi}\left\{\sqrt{p_z^2+m_q^2}\left[1+\mathrm{e}^{\beta\left(\sqrt{p_z^2+m_q^2}\pm\mu\right)}\right]\right\}^{-1}, \tag{114}$$

the thermal part of (106) now reads

$$\begin{aligned} V_{\mathrm{eff}}^{\mathrm{th}} \sim & -\frac{2N_c}{\beta}\sum_f \int \frac{\mathrm{d}^3\mathbf{p}}{(2\pi)^3} \ln\left[1+\mathrm{e}^{-\beta\left(\sqrt{\mathbf{p}^2+m_q^2}\pm\mu\right)}\right] \\ & + \frac{N_c}{4\pi}(q_f B)^2 \sum_f \int \frac{\mathrm{d}p_z}{2\pi}\left\{\sqrt{p_z^2+m_q^2}\left[1+\mathrm{e}^{\beta\left(\sqrt{p_z^2+m_q^2}\pm\mu\right)}\right]\right\}^{-1} + \mathscr{O}(B^4). \end{aligned} \tag{115}$$

where $\mathbf{p}^2 = p_\perp^2 + p_z^2$. The effective potential in the limit of small B can now be written as the sum of a B-independent part,

$$\begin{aligned} V_{\mathrm{eff}}|_{B=0} = & \frac{1}{2}m^2\phi_0^2 + \frac{\lambda}{4!}\phi_0^4 - h\phi_0 + \frac{N_c}{16\pi^2}m_q^4 \sum_f \left[\ln\frac{\Lambda^2}{m_q^2} + \frac{3}{2}\right] \\ & - \frac{2N_c}{\beta}\sum_f \int \frac{\mathrm{d}^3\mathbf{p}}{(2\pi)^3}\left\{\ln\left[1+\mathrm{e}^{-\beta\left(\sqrt{\mathbf{p}^2+m_q^2}-\mu\right)}\right] + \ln\left[1+\mathrm{e}^{-\beta\left(\sqrt{\mathbf{p}^2+m_q^2}+\mu\right)}\right]\right\}, \end{aligned} \tag{116}$$

and a B-dependent part that vanishes when $B \to 0$:

$$V_B = \frac{1}{2}B^2 + \sum_f (q_f B)^2\left[\frac{2}{3}\left(\ln\frac{\Lambda^2}{2|q_f B|}+1\right) + \frac{N_c}{4\pi}\int \frac{\mathrm{d}p_z}{2\pi}\left\{\sqrt{p_z^2+m_q^2}\left[1+\mathrm{e}^{\beta\left(\sqrt{p_z^2+m_q^2}\pm\mu\right)}\right]\right\}^{-1}\right] + \mathscr{O}(B^4). \tag{117}$$

We will also need the $T \to 0$ limit of Eq. (106). The thermal part of the effective potential becomes

$$V_{\mathrm{eff}}^{\mathrm{thermal}} = -\frac{N_c}{2\beta\pi}\sum_{f=u,d}\sum_{l=0}^\infty |q_f B|\alpha_l \int_{-\infty}^\infty \frac{\mathrm{d}p_z}{2\pi}\left\{\ln\left[1+\mathrm{e}^{-\beta\left(\sqrt{p_z^2+M_l^2}-\mu_f\right)}\right] + \ln\left[1+\mathrm{e}^{-\beta\left(\sqrt{p_z^2+M_l^2}+\mu_f\right)}\right]\right\} \tag{118}$$

$$\to^{\beta\to\infty} -\sum_{f,l}\frac{N_c|q_f B|\alpha_l}{(2\pi)^2}\int \mathrm{d}p_z\Big[\theta\left(\mu_f - \sqrt{p_z^2+M_l^2}\right)\left(\mu_f - \sqrt{p_z^2+M_l^2}\right) \tag{119}$$

$$+\theta\left(-\mu_f - \sqrt{p_z^2+M_l^2}\right)\left(-\mu_f - \sqrt{p_z^2+M_l^2}\right)\Big] \tag{120}$$

$$= -\sum_{f,l}\frac{N_c|q_f B|\alpha_l}{(2\pi)^2}\int \mathrm{d}p_z\,\theta\left(|\mu_f| - \sqrt{p_z^2+M_l^2}\right)\left(|\mu_f| - \sqrt{p_z^2+M_l^2}\right) \tag{121}$$

$$= -\sum_{f,l}\frac{2N_c|q_f B|\alpha_l}{(2\pi)^2}\int_0^{p_F^l} \mathrm{d}p_z\left(|\mu_f| - \sqrt{p_z^2+M_n^2}\right) \tag{122}$$

where θ is the step function. The sum over l now runs over all values that satisfy $\mu_f^2 > p_z^2 + M_l^2$, and p_F^l is the Fermi-wavenumber $p_F^l = \sqrt{\mu_f^2 - M_l^2}$. After performing the integral over p_z, we get the following expression:

$$V_{\text{eff}}^{\text{thermal}} = -\sum_{f,l} \frac{N_c |q_f B| \alpha_l}{(2\pi)^2} \left\{ 2|\mu_f| p_F^l - M_l^2 \left[y_l \sqrt{1+y_l^2} + \log\left(y_l + \sqrt{1+y_l^2} \right) \right] \right\}, \tag{123}$$

where $y_l = p_f^l / M_l = \sqrt{\mu_f^2 / M_l^2 - 1}$.

In the vacuum, $T = \mu_u = \mu_d = B = 0$, we have $f_\pi = \phi_0$, where $f_\pi = 93$ MeV is the pion decay constant [19]. From the tree level potential, the four independent parameters of the model, m^2, λ, g and h can be related to physical quantities as follows:

$$\begin{aligned} m^2 &= \frac{1}{2}\left(3m_\pi^2 - m_\sigma^2\right), \\ \lambda &= \frac{3(m_\sigma^2 - m_\pi^2)}{f_\pi^2}, \\ g &= \frac{m_q}{f_\pi}, \\ h &= f_\pi m_\pi^2. \end{aligned} \tag{124}$$

Matching parameters at tree level when working at one-loop order in the effective potential, as in eqs. (124) is commonly done in the literature. However, as is discussed in [20], this is not quite correct, since the expressions for the sigma and pion masses, in terms of the parameters of the model, are modified at one-loop order. With this approximation, the minimum of the effective potential in the vacuum is dependent on the renormalization scale Λ. Since we require that the minimum remains at $\phi_0 = f_\pi$, this fixes Λ at a particular value:

$$\left.\frac{\mathrm{d}V_{\text{eff}}(\phi_0)}{\mathrm{d}\phi_0}\right|_{\phi_0 = f_\pi} = \left.\frac{\mathrm{d}V_0(\phi_0)}{\mathrm{d}\phi_0}\right|_{\phi_0 = f_\pi} + \frac{gN_c}{2\pi^2} m_q^3 \left[\ln\frac{\Lambda^2}{m_q^2} + 1 \right] = 0. \tag{125}$$

Since the tree-level potential already has its minimum at $\phi_0 = f_\pi$, the first term vanishes, and the condition on Λ is

$$\ln\frac{\Lambda^2}{m_q^2} + 1 = 0, \tag{126}$$

or $\Lambda = \mathrm{e}^{-\frac{1}{2}} m_q = \mathrm{e}^{-\frac{1}{2}} g f_\pi$.

Determining the values of the input parameters m_q and m_σ is not trivial. m_q, the effective quark mass, does not correspond directly to a measurable physical quantity. It can be related to the value of the quark condensate in the vacuum [23], which, although not measurable, can, in principle, be computed in lattice simulations. A reasonable estimate is 300 MeV [24], about one third of the mass of a nucleon. m_σ is, in principle, a measurable physical quantity. However, several candidate scalar particles have been observed experimentally, and it is not clear which one should be identified with the σ particle [21]. In some sense, therefore, the sigma mass can be regarded as a free parameter of the model. We will, somewhat arbitrarily, use the value $m_\sigma = 2m_q = 600$ MeV, as is commonly practice in the literature. In the closely related NJL model, the sigma mass is fixed at this value.

Since up and down quarks are not quite massless, pions have finite but relatively small masses of approximately 140 MeV, earning them the name pseudo-Goldstone bosons. Had the up and down quarks been massless, the pions would have been exact massless Goldstone bosons. In [1], the pion masses were set to zero, which is known as the chiral limit. Here, we will focus on the physical point, setting $m_\pi = 140$ MeV.

In the following, we will set $N_c = 3$, as is the case in QCD. We will work with a finite quark chemical potential $\mu = \frac{1}{2}(\mu_d + \mu_u) = \frac{1}{3}\mu_B$, where μ_B is the baryon chemical potential, and set the isospin chemical potential $\mu_I = \frac{1}{2}(\mu_d - \mu_u)$ to zero. The quark charges are fixed at $q_u = \frac{2}{3}|e|$, $q_d = -\frac{1}{3}|e|$, with e the electron charge.

6. The effective potential using tree-level parameter matching

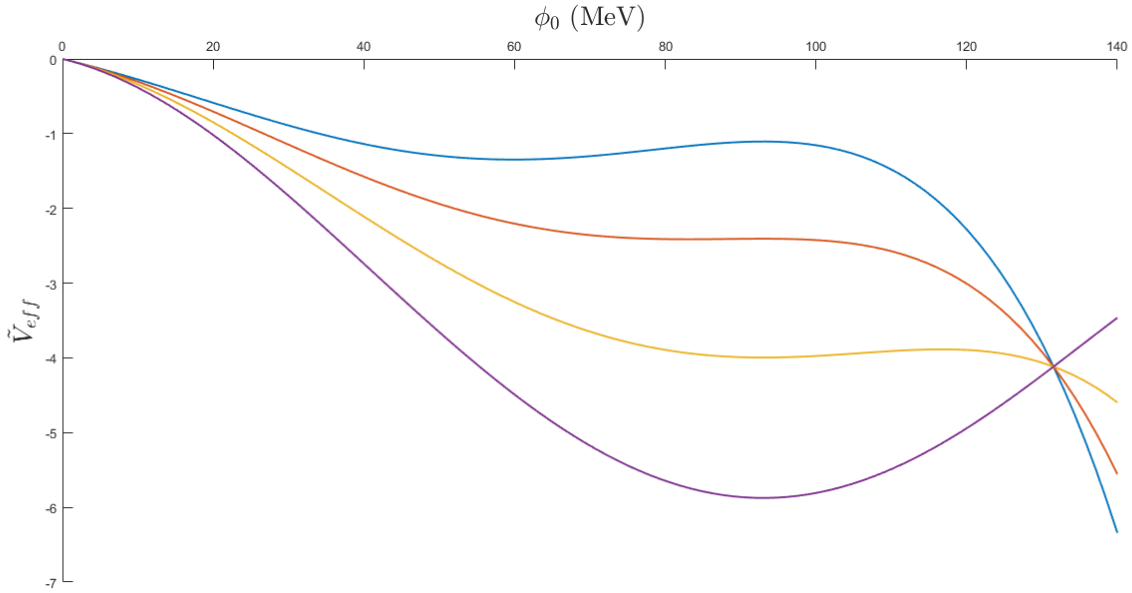

Figure 2: The normalized effective potential $\tilde{V}_{\text{eff}}$ at $\mu = T = B = 0$ using tree-level matching of parameters. The different curves correspond to different choices of the sigma mass, with blue, red yellow and purple corresponding to $m_\sigma = 400$, 500, 600 and 700 MeV respectively.

Using the tree level matching prescription as described above, the effective potential in vacuum was calculated for different choices of the sigma mass, and the plots in figure 2 were produced. As can be seen, condition (126) is not sufficient to secure a minimum at $\phi_0 = f_\pi$ at low values of m_σ. Instead the potential acquires a local maximum at this point. This suggests that the tree-level matching prescription, although commonly employed in model calculations, is perhaps not to be trusted. We will, therefore, make sure to take into account loop corrections before matching parameters.

7. Consistent parameter fixing

When calculating the effective potential at one loop, it is common practice to match parameters at tree level, equating the physical sigma mass to $m_\sigma = m^2 + \frac{\lambda}{2}\phi_0^2$ and so on, with ϕ_0 the minimum

of the tree-level potential. However, this is inconsistent, as the masses and coupling constants receive radiative corrections at this order and depend on the renormalization scale Λ. Matching at tree level is only consistent if one uses the on-shell renormalization scheme, where the counterterms are chosen so as to exactly cancel the loop corrections. Since we have used the $\overline{\text{MS}}$ scheme in calculating the effective potential, we should use the running couplings $m^2_{\overline{\text{MS}}}$, $\lambda_{\overline{\text{MS}}}$ etc. in our calculations. We will calculate these by determining the counterterms in the on-shell scheme, and using the relations between the couplings in the two schemes.

7.1. On-shell renormalization

The bare (Minkowskian) Lagrangian of the QM model reads

$$\mathscr{L} = \frac{1}{2}\left[(\partial_\mu \sigma_B)^2 + (\partial_\mu \vec{\pi}_B)^2\right] - \frac{1}{2}m_B^2\left(\sigma_B^2 + \vec{\pi}_B^2\right) - \frac{\lambda_B}{24}\left(\sigma_B^2 + \vec{\pi}_B^2\right) + h_B\sigma_B + \overline{\psi}_B\left[\partial\!\!\!/ - g_B(\sigma_B + i\gamma_5\vec{\tau}\cdot\vec{\pi}_B)\right]\psi_B. \tag{127}$$

We now define the renormalized quantities

$$\sigma_B^2 = Z_\sigma\sigma^2 = (1+\delta Z_\sigma)\sigma^2, \tag{128}$$
$$\pi_{iB}^2 = Z_\pi\pi_i^2 = (1+\delta Z_\pi)\pi_i^2, \tag{129}$$
$$\bar{\psi}_B\psi_B = Z_\psi\bar{\psi} = (1+\delta Z_\psi)\bar{\psi}\psi, \tag{130}$$
$$m_B^2 = Z_m m^2 = m^2 + \delta m^2, \tag{131}$$
$$\lambda_B = Z_\lambda\lambda = \lambda + \delta\lambda, \tag{132}$$
$$g_B^2 = Z_g g^2 = g^2 + \delta g^2, \tag{133}$$
$$h_B = Z_h h = h + \delta h, \tag{134}$$

where the quantities on the left-hand side are the bare ones appearing in eq. (127). After shifting the field, $\sigma = \phi_0 + \tilde{\sigma}$, the Lagrangian reads

$$\begin{aligned}\mathscr{L} = &-\frac{1}{2}m^2\phi_0^2 - \frac{\lambda}{24}\phi_0^4 + h\phi_0 + \frac{1}{2}\left[(\partial_\mu\tilde{\sigma})^2 + (\partial_\mu\vec{\pi}^2\right] - \frac{1}{2}m_\sigma^2\tilde{\sigma}^2 - \frac{1}{2}m_\pi^2\vec{\pi}^2 - \frac{\lambda\phi_0}{6}\left(\tilde{\sigma}^3 + \tilde{\sigma}\vec{\pi}^2\right) - \frac{\lambda}{24}\left(\tilde{\sigma}^2 + \vec{\pi}^2\right)^2 \\ &+ \left(h - m_\pi^2\phi_0\right)\tilde{\sigma} + \overline{\psi}\left(i\partial\!\!\!/ - m_q\right)\psi - g\overline{\psi}\left[\tilde{\sigma} + i\gamma_5\vec{\tau}\cdot\vec{\pi}\right]\psi,\end{aligned} \tag{135}$$

where the field-dependent masses are

$$m_\sigma^2 = m^2 + \frac{\lambda}{2}\phi_0^2, \tag{136}$$
$$m_\pi^2 = m^2 + \frac{\lambda}{6}\phi_0^2, \tag{137}$$
$$m_q = g\phi_0, \tag{138}$$

We further define

$$m_{\sigma,B}^2 = m_\sigma^2 + \delta m_\sigma^2, \tag{139}$$
$$m_{\pi,B}^2 = m_\pi^2 + \delta m_\pi^2, \tag{140}$$
$$m_{q,B} = m_q + \delta m_q. \tag{141}$$

The above renormalization constants are dependent on the ones in Eqs. (128)–(134).

The pion decay constant f_π can be related to these quantities via the Goldberger-Treiman relation:

$$m_q = g_\pi f_\pi, \tag{142}$$

where g_π is the pion-quark coupling constant. At tree level, $g_\pi = g$, and so we can identify the minimum of the potential with the pion decay constant at tree level via eq. (138). Inverting eqs. (136)-(138), we obtain

$$m^2 = -\frac{1}{2}\left(m_\sigma^2 - 3m_\pi^2\right), \tag{143}$$

$$\lambda = 3\frac{m_\sigma^2 - m_\pi^2}{f_\pi^2}, \tag{144}$$

$$g = \frac{m_q}{f_\pi}. \tag{145}$$

The prescription in the on-shell renormalization scheme is to choose the renormalization constants such that the above relations hold at any given order in perturbation theory, when m_σ, m_π and m_q are identified with the physical masses of the particles, defined as the real part of the poles of the propagators. The propagator for the renormalized sigma field is

$$G_\sigma(p) = \frac{i}{Z_\sigma(p^2 - Z_{m\sigma}m_\sigma^2)}. \tag{146}$$

A Taylor expansion to leading order in δZ_σ, δm_σ^2, gives

$$G_\sigma(p^2) \approx \frac{i}{p^2 - m_\sigma^2} + \frac{i}{p^2 - m_\sigma^2} i\left[\delta Z_\sigma(p^2 - m_\sigma^2) - \delta m_\sigma^2\right]\frac{i}{p^2 - m_\sigma^2}. \tag{147}$$

At one loop, the propagator becomes

$$\begin{aligned} G_\sigma(p^2) &= \frac{i}{p^2 - m_\sigma^2}\left\{1 + \frac{i}{p^2 - m_\sigma^2}\left[i\delta Z_\sigma(p^2 - m_\sigma^2) - i\delta m_\sigma^2 + \Sigma_\sigma(p^2)\right]\right\} \\ &\approx \frac{i}{p^2 - m_\sigma^2 + \delta Z_\sigma(p^2 - m_\sigma^2) - \delta m_\sigma^2 - i\Sigma_\sigma(p^2)}, \end{aligned} \tag{148}$$

where $\Sigma_\sigma(p^2)$ is the one-loop contribution to the self-energy of the sigma particle. Similarly, we get for the pions

$$G_\pi(p^2) = \frac{i}{p^2 - m_\pi^2 + \delta Z_\pi(p^2 - m_\pi^2) - \delta m_\pi^2 - i\Sigma_\pi(p^2)}. \tag{149}$$

The fermion propagator is given by

$$S(p^2) = \frac{i}{\sqrt{Z_\psi}(\not{p} - m_q) - \delta m_q}. \tag{150}$$

In the large-N_c approximation there are no one-loop diagrams contributing to the self-energy of the quarks, so the renormalization constants Z_ψ and Z_{m_q} are equal to unity at this order.

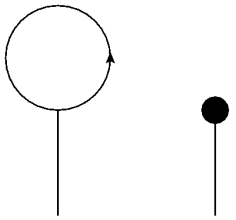

Figure 3: Tadpole diagram with corresponding counterterm diagram

7.2. n-point functions

We begin by evaluating the one-point function of the sigma field. In the large-N_c approximation at one loop, there is one diagram contributing to this, along with one counterterm diagram (Figure 3), which contributes the term $i\delta t$. The one-point function can be written

$$\Gamma^{(1)} = i(h - m_\pi^2 f_\pi) + i\delta t - (-ig)\int \frac{\mathrm{d}^4 q}{(2\pi)^4}\mathrm{Tr}\frac{i(\not{q} + m_q)}{q^2 - m_q^2}, \tag{151}$$

where we have defined $\delta t = \delta(h - m_\pi^2 f_\pi) = \delta h - \delta m_\pi^2 f_\pi - m_\pi^2 \delta f_\pi$. The first term in (151) vanishes identically. After taking the trace we are left with

$$\Gamma^{(1)} = i\delta t - 8N_c g m_q \int \frac{\mathrm{d}^4 q}{(2\pi)^4}\frac{1}{q^2 - m_q^2} \equiv i\delta t - 8N_c g m_q I_1(m_q^2) \tag{152}$$

where we used the fact that the gamma matrices are traceless. A factor of two comes from the sum over quark flavors, a factor of four from the sum over spinor indices, and a factor of N_c from the sum over colors.

In the large-N_c approximation, there are two diagrams contributing to the sigma self-energy, shown in Figure 4, along with two counterterm diagrams. The contribution from diagram *a* is given by

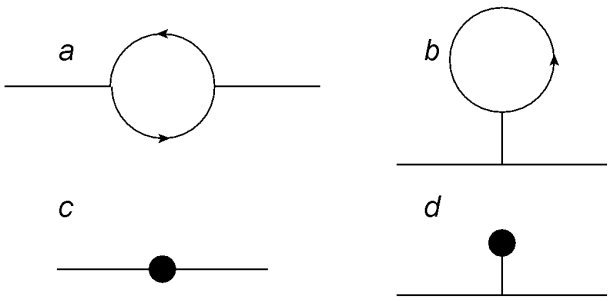

Figure 4: The diagrams contributing to the self-energy of the sigma.

$$\Sigma_\sigma^1(p^2) = -g^2\mathrm{Tr}\int \frac{\mathrm{d}^4 q}{(2\pi)^4}\frac{(\not{q} + \not{p} + m_q)(\not{q} + m_q)}{\left[(q+p)^2 - m_q^2\right]\left[q^2 - m_q^2\right]}. \tag{153}$$

The numerator of the integrand can be written as

$$\frac{1}{2}\left[(q+p)^2 - m_q^2\right] + \frac{1}{2}(q^2 - m_q^2) - \frac{1}{2}(p^2 - 4m_q^2) + m_q(2\not{q} + \not{p}). \tag{154}$$

The last term vanishes after taking the trace. The second term in (154) gives the same integral as the first after shifting the integration variable. We get

$$\Sigma^1_\sigma(p^2) = -8g^2N_c\left[I_1(m_q^2) - \frac{1}{2}(p^2-4m_q^2)I_2(p^2,m_q^2)\right], \tag{155}$$

where

$$I_2(p^2,m^2) = \int \frac{\mathrm{d}^4q}{(2\pi)^4}\frac{1}{[(q+p)^2-m^2]\,[q^2-m^2]}. \tag{156}$$

The contribution from the second diagram is

$$\Sigma^2_\sigma = -(-\frac{1}{2}i\lambda\phi_0)\frac{i}{-m_\sigma^2}(-ig)\mathrm{Tr}\int\frac{\mathrm{d}^4q}{(2\pi)^4}\frac{i(\not{q}+m_q)}{q^2-m_q^2} = \frac{4gN_c\lambda\phi_0}{m_\sigma^2}\int\frac{\mathrm{d}^4q}{(2\pi)^4}\frac{m_q}{q^2-m_q^2} = \frac{4gN_c\lambda\phi_0 m_q}{m_\sigma^2}I_1(m_q^2). \tag{157}$$

Diagram c contributes a term

$$i\delta Z_\sigma(p^2-m_\sigma^2) - i\delta m_\sigma^2, \tag{158}$$

and from diagram d we get

$$-\frac{1}{2}i\lambda\phi_0\frac{-i}{m_\sigma^2}i\delta t = -\frac{\lambda\phi_0}{2m_\sigma^2}i\delta t \tag{159}$$

The diagrams contributing to the pion self-energy are shown in Figure 5. For diagram a, we have

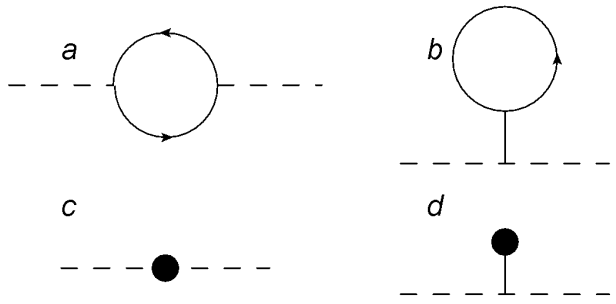

Figure 5: The diagrams contributing to the self-energy of the pions

$$\Sigma^1_\pi(p^2) = -g^2\mathrm{Tr}\int\frac{\mathrm{d}^4q}{(2\pi)^4}\frac{i\gamma_5(\not{q}+\not{p}+m_q)i\gamma_5(\not{q}+m_q)}{\left[(q+p)^2-m_q^2\right]\left[q^2-m_q^2\right]}. \tag{160}$$

After anticommuting the first γ_5 one step to the right, the numerator of the integrand reads

$$\begin{aligned} &i^2(-\not{q}-\not{p}+m_q)(\not{q}+m_q) = q^2+qp+m\not{p}-m^2 \\ &= \frac{1}{2}\left[(q+p)^2-m^2\right]+\frac{1}{2}(q^2-m^2)-\frac{1}{2}p^2+m\not{p}. \end{aligned} \tag{161}$$

We then get

$$\Sigma_\pi^1(p^2) = -8g^2N_c\left[I_1(m_q^2) - \frac{1}{2}p^2 I_2(p^2, m_q^2)\right]. \tag{162}$$

The second contribution is the same as for the sigma, up to a factor of $1/3$ stemming from the lower symmetry of the diagram.

$$\Sigma_\pi^2(p^2) = -\frac{4gN_c\lambda\phi_0 m_q}{3m_\sigma^2} I_1(m_q^2). \tag{163}$$

The counterterm diagrams contribute

$$i\delta Z_\sigma(p^2 - m_\sigma^2) - i\delta m_\sigma^2 - \frac{\lambda\phi_0}{6m_\sigma^2} i\delta t. \tag{164}$$

We will also need the quark-antiquark-pion three-point function. In the large-N_c approximation there are no one-loop diagrams contributing to this, so it is simply given by its tree-level value multiplied by

$$\sqrt{Z_{g_\pi^2}}\sqrt{Z_\pi} \approx 1 + \frac{\delta g_\pi^2}{2g_\pi^2} + \frac{1}{2}\delta Z_\pi. \tag{165}$$

7.3. renormalization conditions

For the minimum of the potential to remain at $\phi_0 = f_\pi$ at one-loop order, the one-point function of the $\tilde{\sigma}$ field must vanish. This gives

$$i\delta t - 8N_c g m_q I_1 = 0. \tag{166}$$

We further require the sigma and pion propagators to have poles at $p^2 = m_\sigma^2$, $p^2 = m_\pi^2$ respectively, with unit residue. This means that the parameters m_σ, m_π will correspond to the physical masses of these particles. The inverse propagator of the sigma is

$$p^2 - m_\sigma^2 + \delta Z_\sigma(p^2 - m_\sigma^2) - \delta m_\sigma - i\Sigma_\sigma(p^2), \tag{167}$$

where

$$\Sigma_\sigma(p^2) = -8g^2N_c\left[I_1 - \frac{1}{2}(p^2 - 4m_q^2)I_2(p^2, m_q^2)\right] + \frac{\lambda\phi_0}{2m_\sigma^2}\left[8N_c g m_q I_1 - i\delta t\right] \tag{168}$$

The last bracket vanishes by eq. (166). We then get

$$\delta m_\sigma^2 = -i\Sigma_\sigma(m_\sigma^2) = 8ig^2N_c\left[I_1 - \frac{1}{2}(m_\sigma^2 - m_q^2)I_2(m_\sigma^2)\right] \tag{169}$$

The residue of the pole equals one if

$$\frac{\partial}{\partial p^2}\left[p^2 - m_\sigma^2 + \delta Z_\sigma(p^2 - m_\sigma^2) - \delta m_\sigma - i\Sigma_\sigma(p^2)\right]|_{p^2=m_\sigma^2} = 1, \tag{170}$$

giving

$$\delta Z_\sigma = i\frac{\mathrm{d}}{\mathrm{d}p^2}\Sigma_\sigma(p^2)|_{p^2=m_\sigma^2} = 4ig^2N_c\left[I_2(m_\sigma^2) + (m_\sigma^2 - 4m_q^2)\frac{\partial}{\partial p^2}I_2(p^2)|_{p^2=m_\sigma^2}\right]. \tag{171}$$

Similarly, we get for the pions

$$\delta m_\pi^2 = 8ig^2 N_c \left[I_1 - \frac{1}{2} m_\pi^2 I_2(m_\pi^2) \right], \tag{172}$$

$$\delta Z_\pi = 4ig^2 N_c \left[I_2(m_\pi^2) + m_\pi^2 \frac{\partial}{\partial p^2} I_2(p^2, m_q^2)|_{p^2=m_\pi^2} \right]. \tag{173}$$

We further require that the pion-quark-antiquark three-point function takes its tree-level value. From (165) this implies

$$\delta g_\pi^2 = -g_\pi^2 \delta Z_\pi. \tag{174}$$

The renormalization constants Z_λ and Z_{m^2} can be related to the ones found above via eqs. (143) - (145). We get

$$\delta m^2 = -\frac{1}{2} \left(\delta m_\sigma^2 - 3\delta m_\pi^2 \right), \tag{175}$$

$$\delta \lambda = 3 \frac{\delta m_\sigma^2 - \delta m_\pi^2}{f_\pi^2} - \lambda \frac{\delta f_\pi^2}{f_\pi^2}, \tag{176}$$

$$\delta g^2 = \frac{\delta m_q^2}{f_\pi^2} - g^2 \frac{\delta f_\pi^2}{f_\pi^2}. \tag{177}$$

Using $\delta m_q^2 = 0$ and combining (174) with (176) and (177) gives

$$\delta \lambda = 3 \frac{\delta m_\sigma^2 - \delta m_\pi^2}{f_\pi^2} - \lambda \delta Z_\pi. \tag{178}$$

Using the the above relations along with eqs. (166), (169), (171), (172) and (173), we can write

$$\begin{aligned}
\delta m^2_{\rm OS} &= 8ig^2N_c\left[I_1+\frac{1}{4}(m_\sigma^2-4m_q^2)I_2(m_\sigma^2)-\frac{3}{4}m_\pi^2 I_2(m_\pi^2)\right]\\
&= \frac{4m^2g^2N_c}{(4\pi)^2\varepsilon}+\frac{4g^2N_c}{(4\pi)^2}\left[m^2\log\frac{\Lambda^2}{m_q^2}-2m_q^2-\frac{1}{2}(m_\sigma^2-4m_q^2)F(m_\pi^2)+\frac{3}{2}m_\pi^2F(m_\pi^2)\right], \qquad (179)\\
\delta\lambda_{\rm OS} &= \frac{12ig^2N_c}{f_\pi^2}\left[m_\pi^2I_2(m_\pi^2)-(m_\sigma^2-4m_q^2)I_2(m_\sigma^2)\right]-4ig^2N_c\lambda\left[I_2(m_\pi^2)+m_\pi^2I_2'(m_\pi^2)\right]\\
&= \frac{8N_c}{(4\pi)^2\varepsilon}(\lambda g^2-6g^4)+\frac{12g^2N_c}{(4\pi)^2f_\pi^2}\Bigg\{(m_\sigma^2-4m_q^2)\left[\log\frac{\Lambda^2}{m_q^2}+F(m_\sigma^2)\right]+m_\sigma^2\log\frac{\Lambda^2}{m_q^2}\\
&\quad +m_\sigma^2F(m_\pi^2)+m_\sigma^2m_\pi^2F'(m_\pi^2)-2m_\pi^2\log\frac{\Lambda^2}{m_q^2}-2m_\pi^2F(m_\pi^2)-m_\pi^4F'(m_\pi^2)\Bigg\}, \qquad (180)\\
\delta g^2_{\rm OS} &= -4ig^4N_c\left[I_2(m_\pi^2+m_\pi^2I_2'(m_\pi^2)\right]=\frac{4g^4N_c}{(4\pi)^2\varepsilon}+\frac{4g^4N_c}{(4\pi)^2}\left[\log\frac{\Lambda^2}{m_q^2}+F(m_\pi^2+m_\pi^2F'(m_\pi^2)\right], \qquad (181)\\
\delta Z_{\sigma,\rm OS} &= -\frac{4g^2N_c}{(4\pi)^2\varepsilon}-\frac{4g^2N_c}{(4\pi)^2}\left[\log\frac{\Lambda^2}{m_q^2}+F(m_\sigma^2)+(m_\sigma^2-4m_q^2)F'(m_\sigma^2)\right], \qquad (182)\\
\delta Z_{\pi,\rm OS} &= -\frac{4g^2N_c}{(4\pi)^2\varepsilon}-\frac{4g^2N_c}{(4\pi)^2}\left[\log\frac{\Lambda^2}{m_q^2}+F(m_\pi^2)+m_\pi^2F'(m_\pi^2)\right], \qquad (183)\\
\delta h_{\rm OS} &= -2ig^2N_cm_\pi^2f_\pi\left[I_2(m_\pi^2)+m_\pi^2I_2'(m_\pi^2)\right]\\
&= \frac{2g^2hN_c}{(4\pi)^2\varepsilon}+\frac{2g^2hN_c}{(4\pi)^2}\left[\log\frac{\Lambda^2}{m_q^2}+F(m_\pi^2)+m_\pi^2F'(m_\pi^2)\right], \qquad (184)
\end{aligned}$$

where we have used Eqs. (A.20), (A.26) and (A.29). where the subscript OS is added to emphasize that these are the counterterms in the on-shell scheme. The counterterms in the $\overline{\rm MS}$ scheme are just the divergent parts of the above expressions, i.e.

$$\delta m^2_{\overline{\rm MS}}=\frac{4m^2g^2N_c}{(4\pi)^2\varepsilon}, \qquad (185)$$

etc. The renormalized parameters in the $\overline{\rm MS}$ can be related to those in the on-shell scheme via

$$m_B^2=Z^{\rm OS}_{m^2}m^2_{\rm OS}=Z^{\overline{\rm MS}}_{m^2}m^2_{\overline{\rm MS}}\implies m^2_{\overline{\rm MS}}=\frac{Z^{\rm OS}_{m^2}}{Z^{\overline{\rm MS}}_{m^2}}m^2_{\rm OS}\approx m^2_{\rm OS}+\delta m^2_{\rm OS}-\delta m^2_{\overline{\rm MS}} \qquad (186)$$

and so on. This yields

$$
\begin{aligned}
m^2_{\overline{\rm MS}} &= m^2 + 8ig^2N_c\left[I_1 + \frac{1}{4}(m_\sigma^2 - 4m_q^2)I_2(m_\sigma^2) - \frac{3}{4}m_\pi^2 I_2(m_\pi^2)\right] - \delta m^2_{\overline{\rm MS}} \\
&= m^2 + \frac{4g^2N_c}{(4\pi)^2}\left[m^2\log\frac{\Lambda^2}{m_q^2} - 2m_q^2 - \frac{1}{2}(m_\sigma^2 - 4m_q^2)F(m_\pi^2) + \frac{3}{2}m_\pi^2 F(m_\pi^2)\right], \qquad (187)\\
\lambda_{\overline{\rm MS}} &= \lambda + \frac{12ig^2N_c}{f_\pi^2}\left[m_\pi^2 I_2(m_\pi^2) - (m_\sigma^2 - 4m_q^2)I_2(m_\sigma^2)\right] - 4ig^2N_c\lambda\left[I_2(m_\pi^2) + m_\pi^2 I_2'(m_\pi^2)\right] - \delta\lambda_{\overline{\rm MS}} \\
&= \lambda + \frac{12g^2N_c}{(4\pi)^2 f_\pi^2}\Bigg\{(m_\sigma^2 - 4m_q^2)\left[\log\frac{\Lambda^2}{m_q^2} + F(m_\sigma^2)\right] + m_\sigma^2\log\frac{\Lambda^2}{m_q^2} \\
&\quad + m_\sigma^2 F(m_\pi^2) + m_\sigma^2 m_\pi^2 F'(m_\pi^2) - 2m_\pi^2\log\frac{\Lambda^2}{m_q^2} - 2m_\pi^2 F(m_\pi^2) - m_\pi^4 F'(m_\pi^2)\Bigg\}, \qquad (188)\\
g^2_{\overline{\rm MS}} &= -4ig^4N_c\left[I_2(m_\pi^2 + m_\pi^2 I_2'(m_\pi^2)\right] - \delta g^2_{\overline{\rm MS}} = g^2 + \frac{4g^4N_c}{(4\pi)^2}\left[\log\frac{\Lambda^2}{m_q^2} + F(m_\pi^2 + m_\pi^2 F'(m_\pi^2)\right], \qquad (189)\\
h_{\overline{\rm MS}} &= h - 2ig^2N_c m_\pi^2 f_\pi\left[I_2(m_\pi^2) + m_\pi^2 I_2'(m_\pi^2)\right] - \delta h_{\overline{\rm MS}} \\
&= h + \frac{2g^2hN_c}{(4\pi)^2}\left[\log\frac{\Lambda^2}{m_q^2} + F(m_\pi^2) + m_\pi^2 F'(m_\pi^2)\right], \qquad (190)
\end{aligned}
$$

From the above relations we can extract the RG equations for the running couplings in the $\overline{\rm MS}$ scheme:

$$
\begin{aligned}
\Lambda\frac{{\rm d}m^2}{{\rm d}\Lambda} &= \frac{8g^2N_c}{(4\pi)^2}m^2, \qquad (191)\\
\Lambda\frac{{\rm d}g^2}{{\rm d}\Lambda} &= \frac{8g^4N_c}{(4\pi)^2}, \qquad (192)\\
\Lambda\frac{{\rm d}\lambda^2}{{\rm d}\Lambda} &= \frac{16N_c}{(4\pi)^2}\left[\lambda g^2 - 6g^4\right], \qquad (193)\\
\Lambda\frac{{\rm d}h}{{\rm d}\Lambda} &= \frac{4g^2hN_c}{(4\pi)^2}. \qquad (194)
\end{aligned}
$$

The general solutions to these equations can be expressed as follows:

$$
\begin{aligned}
m^2_{\overline{\rm MS}} &= \frac{m_0^2}{1 - \frac{4g_0^2N_c}{(4\pi)^2}\left[\log\frac{\Lambda^2}{m_q^2} + F(m_\pi^2) + m_\pi^2F'(m_\pi^2)\right]}, \qquad (195)\\
g^2_{\overline{\rm MS}} &= \frac{g_0^2}{1 - \frac{4g_0^2N_c}{(4\pi)^2}\left[\log\frac{\Lambda^2}{m_q^2} + F(m_\pi^2) + m_\pi^2F'(m_\pi^2)\right]}, \qquad (196)\\
\lambda_{\overline{\rm MS}} &= \frac{\lambda_0 - \frac{48g_0^4N_c}{(4\pi)^2}\log\frac{\Lambda^2}{m_q^2}}{\left\{1 - \frac{4g_0^2N_c}{(4\pi)^2}\left[\log\frac{\Lambda^2}{m_q^2} + F(m_\pi^2) + m_\pi^2F'(m_\pi^2)\right]\right\}^2}, \qquad (197)\\
h_{\overline{\rm MS}} &= \frac{h_0}{1 - \frac{4g_0^2N_c}{(4\pi)^2}\left[\log\frac{\Lambda^2}{m_q^2} + F(m_\pi^2) + m_\pi^2F'(m_\pi^2)\right]}, \qquad (198)
\end{aligned}
$$

where m_0^2, g_0^2, λ_0 and h_0 are determined by fitting eqs. (195)- (198) with eqs.(187) - (190), for example, m_0^2 is the value of $m^2_{\overline{\rm MS}}$ at the value of Λ such that $\log\frac{\Lambda^2}{m_q^2}+F(m_\pi^2)+m_\pi^2F'(m_\pi^2)=0$.

We now define $\Delta = g_{\overline{\rm MS}}\phi_{0\overline{\rm MS}}$. Expressed in terms of this, the vacuum part of the effective potential at one loop is

$$V_{\rm eff}^{\rm vac}(\Delta)=\frac{1}{2}m^2(\Lambda)\frac{\Delta^2}{g^2(\Lambda)}+\frac{\lambda(\Lambda)}{24}\frac{\Delta^4}{g^4(\Lambda)}-h(\Lambda)\frac{\Delta}{g(\Lambda)}+\frac{2N_c\Delta^4}{(4\pi)^2}\left[\log\frac{\Lambda^2}{\Delta^2}+\frac{3}{2}\right]. \tag{199}$$

When eqs. (195) - (198) are inserted into (199), all instances of Λ cancel out and we are left with the following expression:

$$V_{\rm eff}^{\rm vac}(\Delta)=\frac{3}{4}m_\pi^2f_\pi^2\left[1-\frac{4m_q^2N_c}{(4\pi)^2f_\pi^2}m_\pi^2F'(m_\pi^2)\right]\frac{\Delta^2}{m_q^2} \tag{200}$$

$$-\frac{1}{4}m_\sigma^2f_\pi^2\left\{1+\frac{4m_q^2N_c}{(4\pi)^2f_\pi^2}\left[\left(1-\frac{4m_q^2}{m_\sigma^2}\right)F(m_\sigma^2)+\frac{4m_q^2}{m_\sigma^2}-F(m_\pi^2)-m_\pi^2F'(m_\pi^2)\right]\right\}\frac{\Delta^2}{m_q^2} \tag{201}$$

$$+\frac{1}{8}m_\sigma^2f_\pi^2\left\{1-\frac{4m_q^2N_c}{(4\pi)^2f_\pi^2}\left[\frac{4m_q^2}{m_\sigma^2}\left(\log\frac{\Delta^2}{m_q^2}-\frac{3}{2}\right)-\left(1-\frac{4m_q^2}{m_\sigma^2}\right)F(m_\sigma^2)+F(m_\pi^2)+m_\pi^2F'(m_\pi^2)\right]\right\}\frac{\Delta^4}{m_q^4} \tag{202}$$

$$-\frac{1}{8}m_\pi^2f_\pi^2\left[1-\frac{4m_q^2N_c}{(4\pi)^2f_\pi^2}m_\pi^2F'(m_\pi^2)\right]\frac{\Delta^4}{m_q^4}-m_\pi^2f_\pi^2\left[1-\frac{4m_q^2N_c}{(4\pi)^2f_\pi^2}m_\pi^2F'(m_\pi^2)\right]\frac{\Delta}{m_q}, \tag{203}$$

$$\tag{204}$$

where f_π, m_σ,m_π and m_q can now be matched with the corresponding physical observables.

7.4. Including a magnetic field

In the large-N_c approximation, the inclusion of an electromagnetic field does not change the renormalization of the quantities considered so far, since diagrams with photon loops are neglected. The only diagram we need to consider is the photon self-energy, shown in figure 6. Assuming one species of fermion (the result generalizes easily to several species), the relevant part of the Lagrangian density is

$$\mathscr{L}_{\rm QED}=\bar\psi_B\left[i\gamma^\mu(\partial_\mu+iq_BA_{\mu B})-m_{qB}\right]\psi_B-\frac{1}{4}F_B^{\mu\nu}F_{\mu\nu B}. \tag{205}$$

We define the renormalized quantities

$$A_{\mu B}=\sqrt{Z_A}A_\mu=(1+\frac{1}{2}\delta Z_A)A_\mu, \tag{206}$$

$$q_BZ_\psi\sqrt{Z_A}=Z_qq=q+\delta q. \tag{207}$$

The bare photon propagator in the Feynman gauge reads

$$G^{\mu\nu}(p)=-\frac{i\eta^{\mu\nu}}{p^2}. \tag{208}$$

It can be shown that (see [22]) the full two-point function of the photon is of the form

$$\frac{-i\eta^{\mu\nu}}{p^2(1-\Pi(p^2))}, \tag{209}$$

where

$$\Pi^{\mu\nu}(p^2) = (p^2\eta^{\mu\nu} - p^\mu p^\nu)\Pi(p^2) \tag{210}$$

is the self-energy of the photon. The two new renormalization constants are fixed by the following conditions:

$$\Pi^{\mu\nu}(p^2 = 0) = 0, \tag{211}$$

$$\Gamma^\mu(p - p' = 0) = \gamma^\mu. \tag{212}$$

The first condition states that the photon self-energy $\Pi^{\mu\nu}(p^2)$ vanishes at $p^2 = 0$, which ensures that the photon propagator has a unit residue at the pole. The second condition states that the photon - fermion -fermion three point function takes its tree-level value at zero momentum exchange, which ensures that the renormalized charge q can be identified with the physical charge of the fermion measured at large distances. We will not carry out the full calculation of Z_q and Z_A, but only sketch the derivation. The full derivation can be found in e.g. [22].

There is a Ward identity which guarantees that $Z_q = Z_\psi$. From Eq. (207), this implies $q_B = Z_A^{-1/2} q$. Thus, we only need to determine Z_A. The one-loop contribution to the photon two-point function is

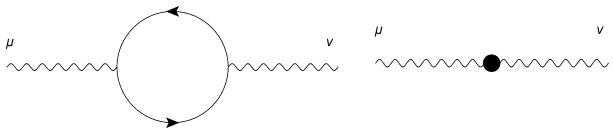

Figure 6: The photon self-energy with counterterm diagram

shown diagrammatically in figure 6, along with the counterterm diagram. The contribution from the loop diagram is given by

$$i\Pi^{\mu\nu}(p) = \sum_f -(-iq_f)^2 \int \frac{\mathrm{d}^4k}{(2\pi)^4} + \mathrm{Tr}\left[\gamma^\mu \frac{i}{\not{k} - m_q}\gamma^\nu \frac{i}{\not{k} + \not{p} - m_q}\right]. \tag{213}$$

The contribution from the counterterm diagram is

$$-i(\eta^{\mu\nu}p^2 - p^\mu p^\nu)\delta Z_A. \tag{214}$$

The integral in (213) can be evaluated in the same way as (153). This is done in [22], and we will not replicate the derivation here. The result is

$$\Pi^{\mu\nu}(p) = (p^2\eta^{\mu\nu} - p^\mu p^\nu)\Pi(p^2), \tag{215}$$

where

$$\Pi(0) = -\frac{q^2}{12\pi^2}\left(\frac{1}{\varepsilon} + \log\frac{\Lambda^2}{m_q^2}\right) \tag{216}$$

This yields the renormalization constants in the on-shell scheme:

$$\delta Z_A^{\mathrm{OS}} = -\delta q^2_{\mathrm{OS}} = -\frac{q^2_{\mathrm{OS}}}{12\pi^2}\left(\frac{1}{\varepsilon} + \log\frac{\Lambda^2}{m_q^2}\right). \tag{217}$$

With several species of fermions, we get

$$\delta Z_A^{\rm OS} = -\sum_f \frac{q_{f\rm OS}^2}{12\pi^2}\left(\frac{1}{\varepsilon}+\log\frac{\Lambda^2}{m_q^2}\right). \tag{218}$$

In the $\overline{\rm MS}$ scheme we then get

$$B^2_{\overline{\rm MS}} = B^2_{\rm OS}\left[1-\frac{N_c}{12\pi^2}\log\frac{\Lambda^2}{m_q^2}\sum_f q_{f\rm OS}^2\right]. \tag{219}$$

and

$$q_{f,\overline{\rm MS}}B_{\overline{\rm MS}} = q_{f,\rm OS}B_{\rm OS}. \tag{220}$$

The effective potential is

$$\begin{aligned} V_{\rm eff} &= \frac{1}{2}m^2\frac{\Delta^2}{g^2}+\frac{\lambda}{4!}\frac{\Delta^4}{g^4}-h\frac{\Delta}{g}+\frac{1}{2}B^2 \\ &+\frac{N_c}{16\pi^2}\sum_f\left\{\left(\ln\frac{\Lambda^2}{2|q_fB|}+1\right)\left[\frac{2(q_fB)^2}{3}+\Delta^4\right]-8(q_fB)^2\zeta^{(1,0)}(-1,x_f)-2|q_fB|\Delta^2\ln x_f\right\}, \end{aligned}$$

where $x_f=\Delta^2/2|q_fB|$.After inserting the $\overline{\rm MS}$ running parameters, we get

$$V_{\rm eff}(\Delta) = \frac{3}{4}m_\pi^2 f_\pi^2\left[1-\frac{4m_q^2N_c}{(4\pi)^2f_\pi^2}m_\pi^2F'(m_\pi^2)\right]\frac{\Delta^2}{m_q^2} \tag{221}$$

$$-\frac{1}{4}m_\sigma^2f_\pi^2\left\{1+\frac{4m_q^2N_c}{(4\pi)^2f_\pi^2}\left[\left(1-\frac{4m_q^2}{m_\sigma^2}\right)F(m_\sigma^2)+\frac{4m_q^2}{m_\sigma^2}-F(m_\pi^2)-m_\pi^2F'(m_\pi^2)\right]\right\}\frac{\Delta^2}{m_q^2} \tag{222}$$

$$+\frac{1}{8}m_\sigma^2f_\pi^2\left\{1+\frac{4m_q^2N_c}{(4\pi)^2f_\pi^2}\left[\left(1-\frac{4m_q^2}{m_\sigma^2}\right)F(m_\sigma^2)-F(m_\pi^2)-m_\pi^2F'(m_\pi^2)\right]\right\}\frac{\Delta^4}{m_q^4} \tag{223}$$

$$-\frac{1}{8}m_\pi^2f_\pi^2\left[1-\frac{4m_q^2N_c}{(4\pi)^2f_\pi^2}m_\pi^2F'(m_\pi^2)\right]\frac{\Delta^4}{m_q^4}-m_\pi^2f_\pi^2\left[1-\frac{4m_q^2N_c}{(4\pi)^2f_\pi^2}m_\pi^2F'(m_\pi^2)\right]\frac{\Delta}{m_q} \tag{224}$$

$$+\frac{N_c}{16\pi^2}\sum_f\left\{\left(\ln\frac{m_q^2}{2|q_fB|}+1\right)\left[\frac{2(q_fB)^2}{3}+\Delta^4\right]-8(q_fB)^2\zeta^{(1,0)}(-1,x_f)-2|q_fB|\Delta^2\ln x_f\right\} \tag{225}$$

8. Numerical results

In figure 7 the effective potential in vacuum is plotted for the same values of the sigma mass as in figure 2, this time using the running parameters found in the previous section. In this case, the potential exhibits a local minimum at $\Delta = 300$ MeV for all values of m_σ. As is discussed in ref. [1], the potential tends to $-\infty$ for large values of Δ. As in [1], we will assume that the local minima seen in figure 7 correspond to the global minimum of the potential when calculated to all orders including the meson fluctuations.

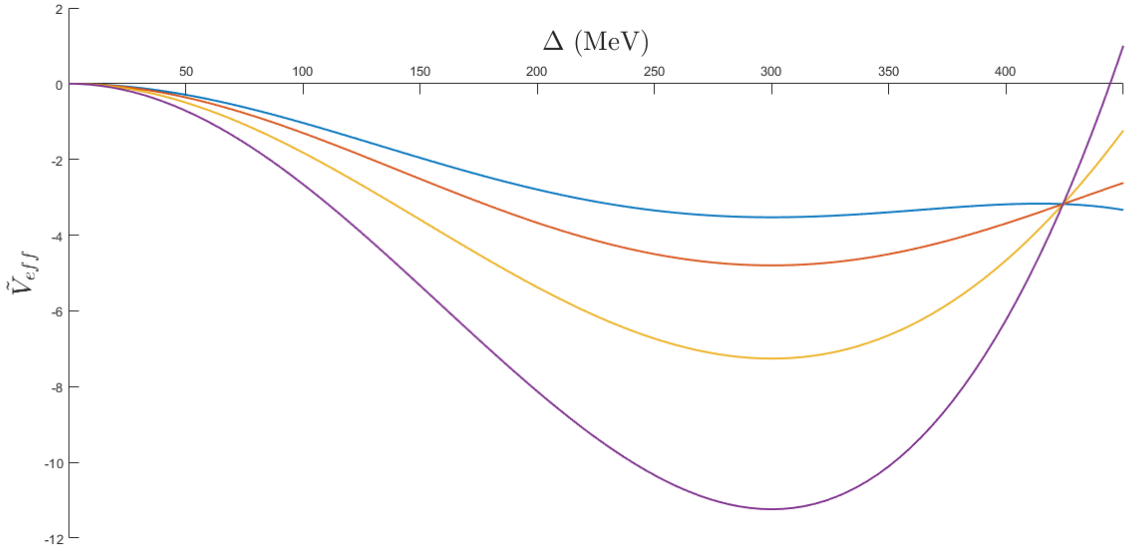

Figure 7: The normalized effective potential $\tilde{V}_{\text{eff}}$ at $\mu = B = T = 0$, using the running $\overline{\text{MS}}$-parameters. The different curves correspond to different choices of the sigma mass, with blue, red yellow and purple corresponding to $m_\sigma = 400$, 500, 600 and 700 MeV respectively.

We will first consider the model in the absence of a magnetic field. In [1], the phase structure of the QM model in the chiral limit was investigated. We will here consider the case of finite pion masses $m_\pi = 140$ MeV, i.e. the physical point. In this case, chiral symmetry is explicitly broken in the Lagrangian, as $h \neq 0$. This means that the expectation value of Δ never vanishes completely. It does, however approach zero at large temperatures and densities, and one can speak of *approximate* chiral symmetry restoration. This type of phase transition is known as a crossover. Figure 8 shows the expectation value of Δ as a function of temperature at $\mu = 0$. The curve has a single inflection point at $T = 175$ MeV, $\Delta = 109$ MeV, which is marked with a red circle. We will use this point to define a *pseudocritical temperature*, characterizing the temperature at which chiral symmetry is approximately restored. Other definitions are possible, such as the point at which Δ reaches a certain fraction of its vacuum value.

Figure 9 shows the phase diagram which was produced by computing the critical temperature, as defined by the inflection point of $\Delta(T)$, for various values of μ. The transition becomes more abrupt as μ is increased, but remains a continuous crossover in the entire phase plane. It may be interesting to consider how things change if vacuum fluctuations are neglected. In this case, the transition was found to be discontinuous at high values of μ. Figure 10 shows Δ plotted as a function of T for $\mu = 250$ MeV. There is a discontinuity at $T = 73$ MeV. The phase diagram which is produced when vacuum fluctuations are excluded is shown in figure 11. There is a critical point at $\mu = 225$ MeV, $T = 90$ MeV, separating the region of smooth crossover from that of a discontinuous transition. Note that defining the pseudocritical temperature as we have done, the phase line remains continuous, since the discontinuity of $\Delta(\mu, T)$ just beyond the critical point coincides with the inflection point just below the critical point.

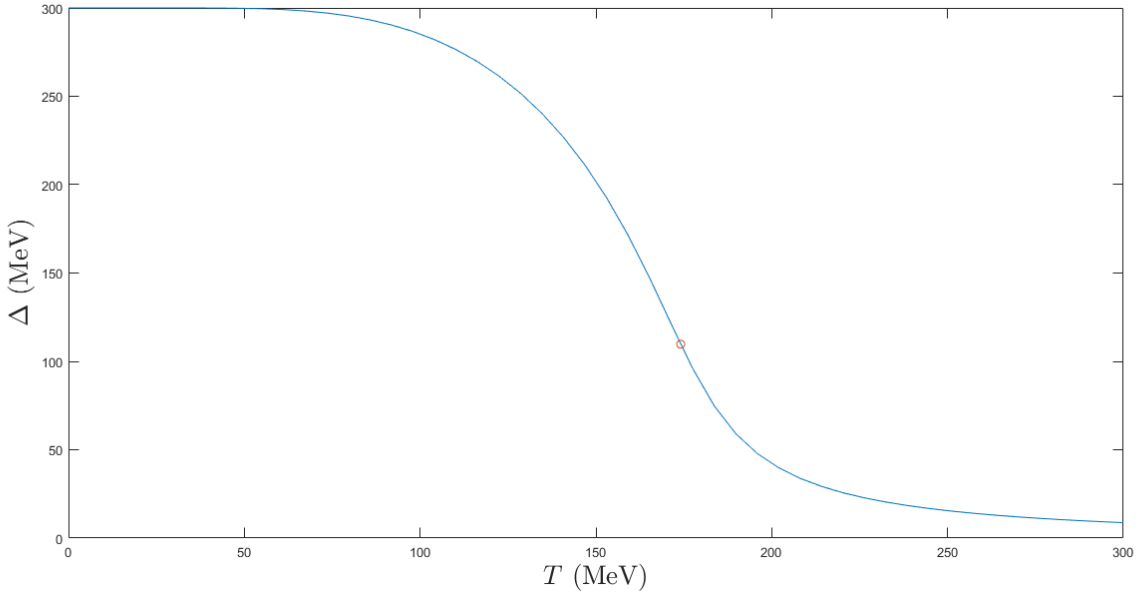

Figure 8: The expectation value of Δ as a function of T, at $\mu = 0$. The red circle marks the inflection point of the curve.

9. Introducing a magnetic field

In figure 12 the normalized effective potential

$$\tilde{V}_{\text{eff}}(\phi_0) \equiv \frac{V_{\text{eff}}(\phi_0) - V_{\text{eff}}(0)}{f_\pi^4} \tag{226}$$

is plotted for three different values of $|eB|$. As the magnetic field increases, the minimum of the potential becomes deeper, and is pushed towards higher values of Δ. Thus, the presence of a magnetic field can be said to enhance the effect of symmetry breaking by increasing the magnitude of the chiral condensate. This is the magnetic catalysis phenomenon mentioned earlier.

In figure 13, the change in Δ is plotted as a function of $|eB|$ for different values of T. The same type of plot was produced in [8] using lattice methods, where it was found that the condensate is a decreasing function of the magnetic field strength for sufficiently high values of T. As figure 13 shows, the quark-meson model does not reproduce this behaviour. Rather, the model exhibits magnetic catalysis at all temperatures.

We will now focus on the case of $T = 0$, with μ and B finite. It turns out that the behavior of the effective potential becomes significantly more complicated when a magnetic field is switched on. Figure 14 shows the expectation value of Δ as a function of μ at $T = 0$ and $|eB| = m_\pi^2$. There are numerous discontinuities. The same plot for $|eB| = 3m_\pi^2$ is shown in figure 15. In this case the jumps are fewer, but larger in magnitude. By numerically differentiating these curves at various values of $|eB|$ and detecting the spikes, a phase diagram can be mapped out. The result is shown in figure 16. The diagram is computed at finite resolution; at infinite resolution the points would coalesce into continuous curves. This method is limited by computational capacity, especially at small values of $|eB|$ where the discontinuities become progressively smaller in magnitude and thus harder to detect numerically.

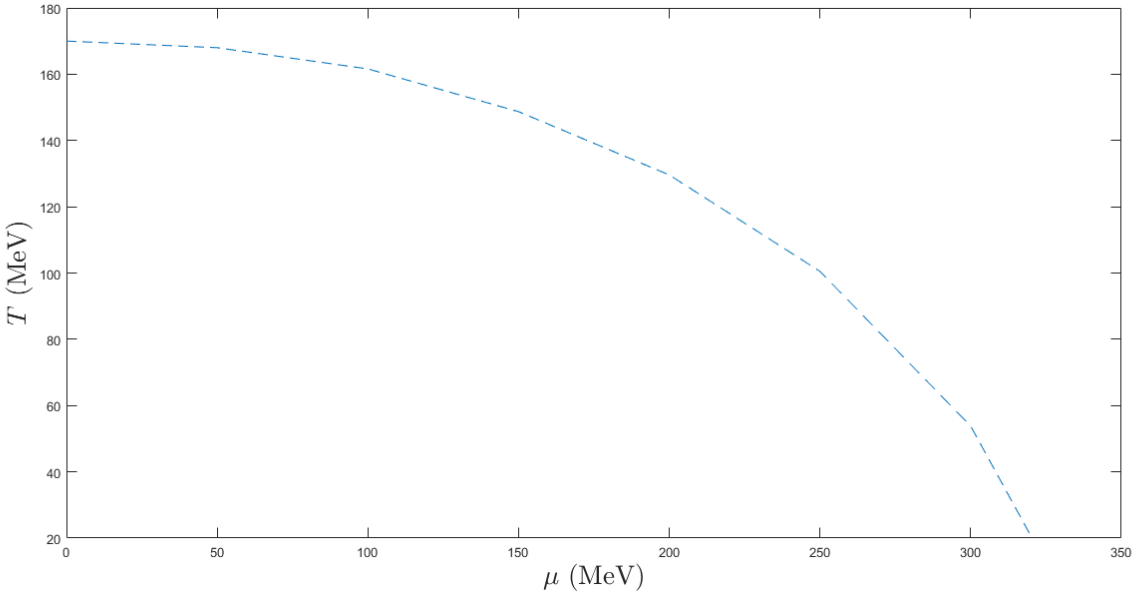

Figure 9: The phase diagram in the μ-T plane at the physical point. The phase transition is a crossover in the entire phase plane, and the critical temperature is defined by the inflection point of Δ as a function of temperature.

However, the qualitative form of the phase diagram can be seen. In [7], the same phase diagram was studied using the two-flavor NJL model. Although different parameters were used (the constituent quark mass was set to 400 MeV, with $m_\sigma = 2m_q = 800$ MeV, the qualitative form of the phase diagram was the same as was found here.

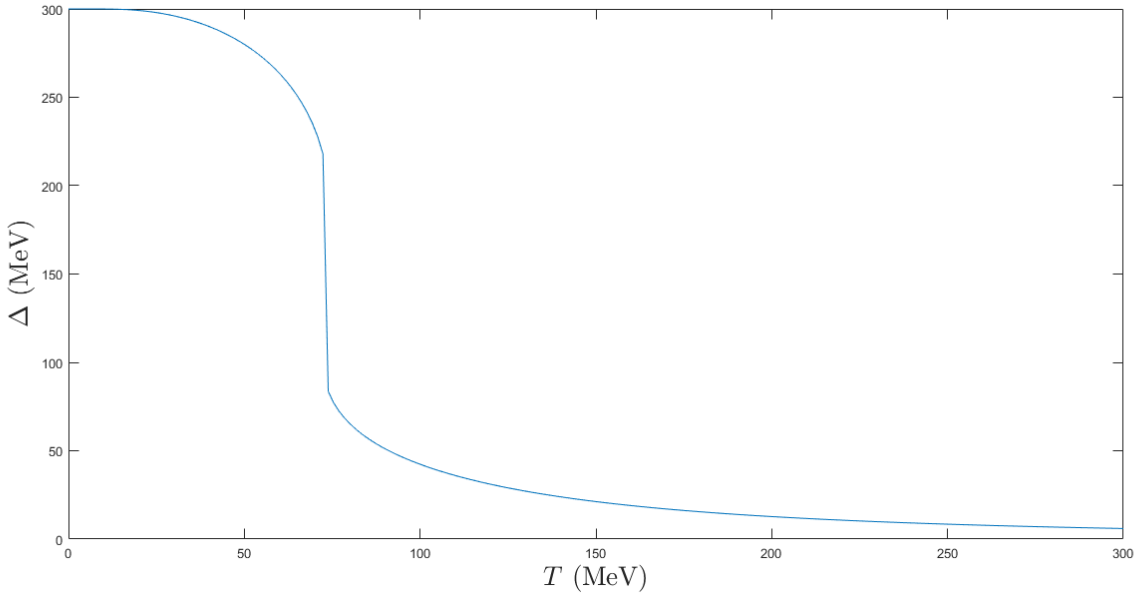

Figure 10: Δ as a function of T for $\mu = 250$ MeV with vacuum fluctuations neglected. There is a discontinuity at $T = 73$ MeV.

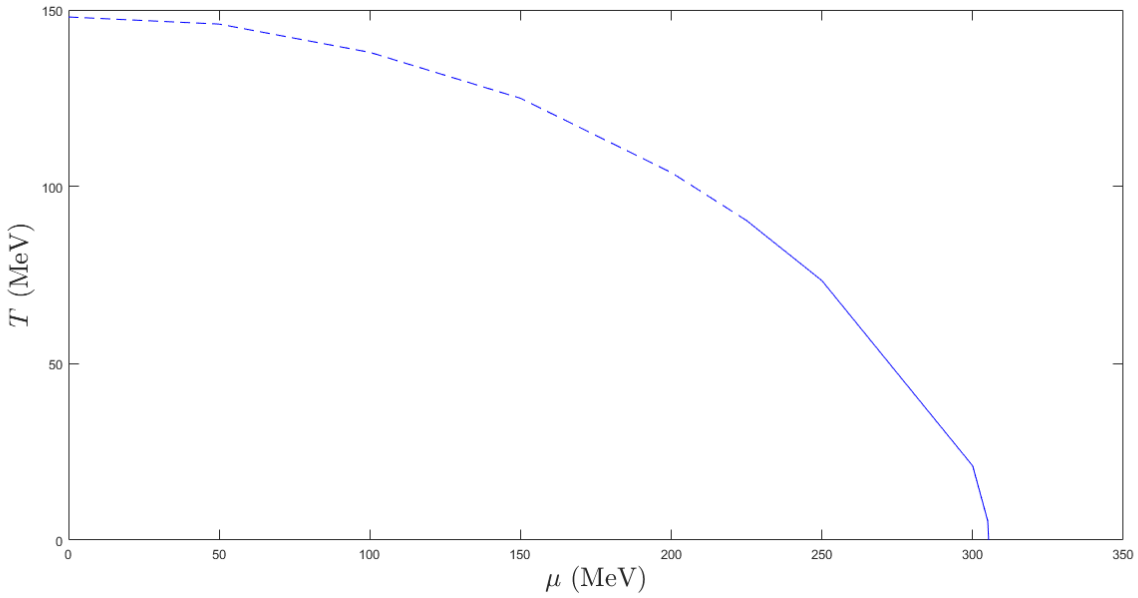

Figure 11: The phase diagram in the μ-T plane with vacuum fluctuations neglected. For low values of μ the transition is a smooth crossover, whereas at high values of μ the transition becomes discontinuous. The critical point is found at $\mu = 225$ MeV, $T = 90$ MeV.

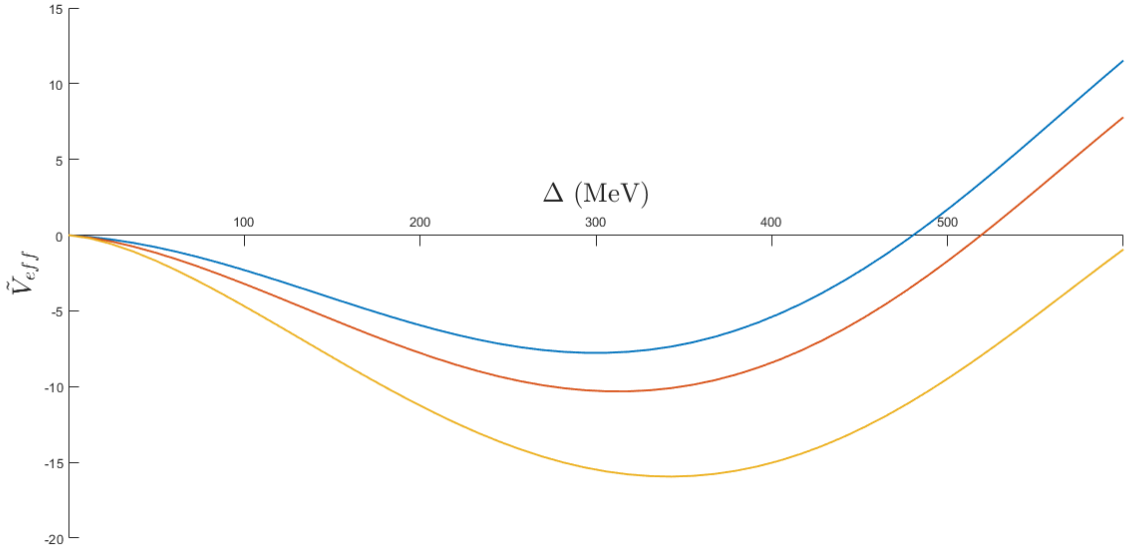

Figure 12: The normalized effective potential $\tilde{V}_{\text{eff}}$ at zero temperature and baryon chemical potential, and three different values of the magnetic field. The blue, red and yellow curves correspond to $|eB| = 0$, $|eB| = 5m_\pi^2$ and $|eB| = 10m_\pi^2$, respectively.

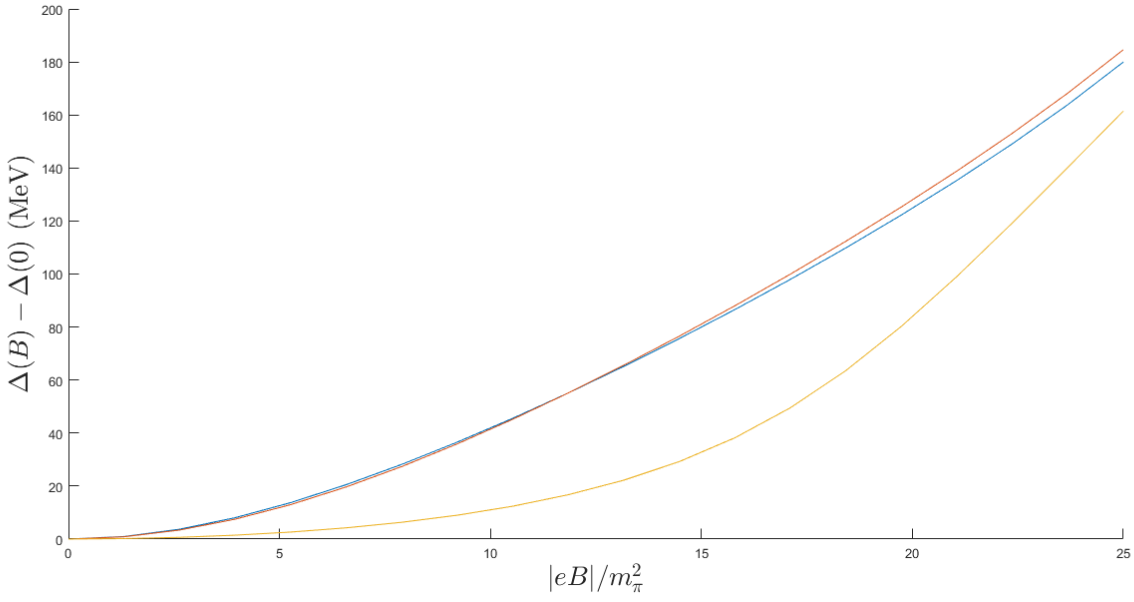

Figure 13: The change in Δ as a function of $|eB|$, plotted for $T = 0$ (blue curve), $T = 100$ MeV (red curve) and $T = 200$ MeV (yellow curve).

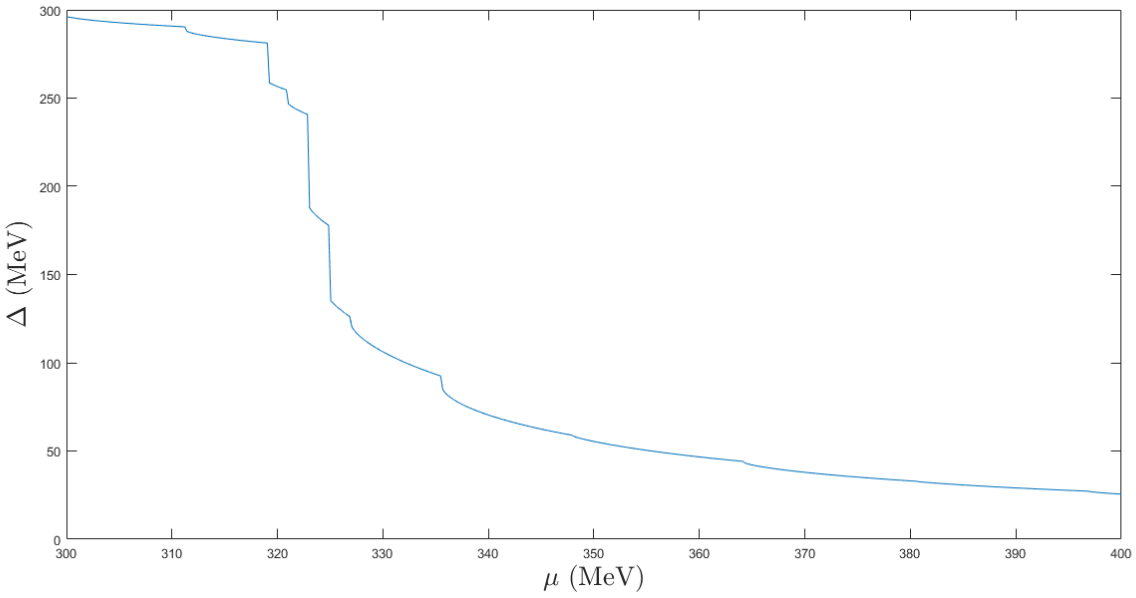

Figure 14: The minimum of the potential as a function of μ at $T = 0$, $|eB| = m_\pi^2$.

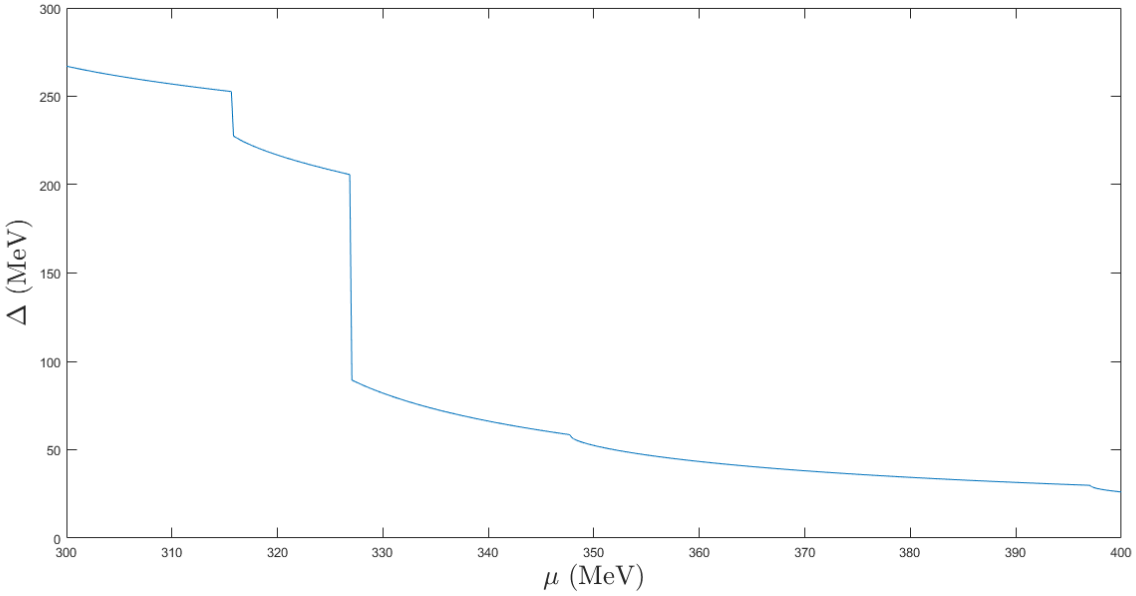

Figure 15: The minimum of the potential as a function of μ at $T = 0$, $|eB| = 3m_\pi^2$.

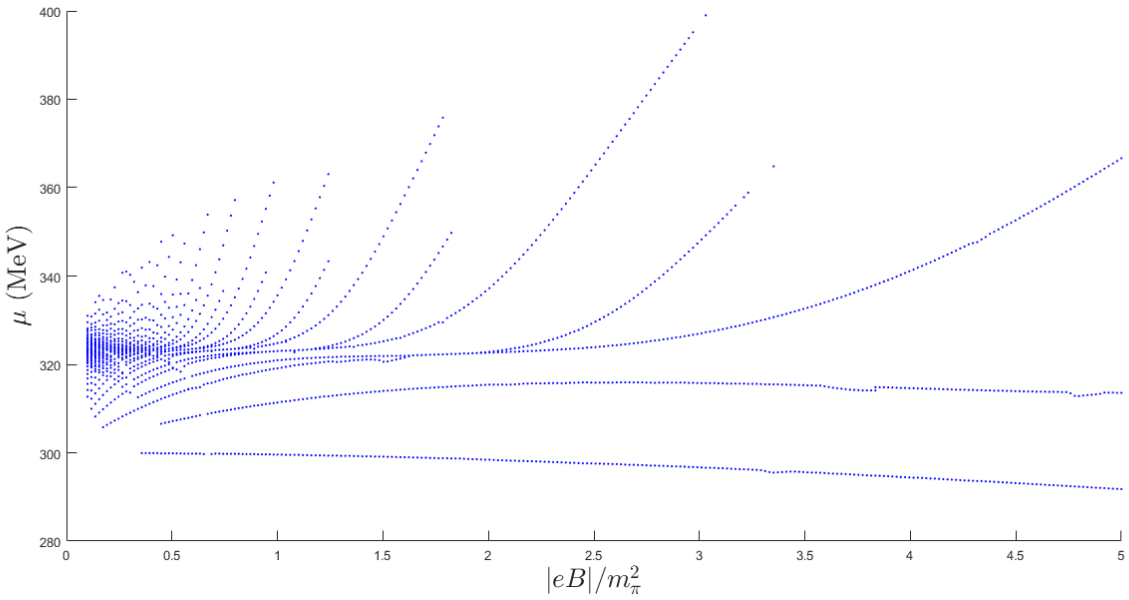

Figure 16: The phase diagram in the B-μ plane at $T = 0$. each point marks a first-order phase transition.

10. Conclusion and outlook

In this thesis we have expanded on the work which was done in [1], in three respects. Firstly, loop corrections were taken into account when the parameters of the model were matched with observable quantities. In [1], it was found that the tree-level matching prescription fails to produce even a local minimum of the effective potential for certain values of the sigma mass. As we have seen, this problem no longer persists when parameter matching is done properly. Secondly, a finite pion mass was incorporated. This turns the chiral phase transition into a crossover, and in order to produce a phase diagram we have to define a pseudocritical temperature.

Thirdly, an external magnetic field was incorporated in the model. As expected, the quark-meson model was found to exhibit magnetic catalysis at all temperatures, in conflict with the currently most reliable lattice results. This may be a consequence of some underlying mechanism not captured by this or any of the other current models. So far, attempts to reproduce inverse magnetic catalysis by modifying the quark-meson model (or its Polyakov loop extension) have been unsuccessful. Possibly, a more sophisticated model may be conceived in the future which accomplishes this.

11. References

[1] S. Grøver, *The phase diagram of the quark-meson model* (attachment)
[2] K. Fukushima, T. Hatsuda, *The phase diagram of dense QCD*, Rept. Prog. Phys. (2011) Phys. 74, 014001.
[3] S. Muroya et.al., *Lattice QCD at Finite Density - An introductory review*, arXiv:hep-lat/0306031
[4] V. Skokov, A. Illarionov, V. Toneev, *Estimate of the magnetic field strength in heavy-ion collisions*, arXiv:0907.1396 [nucl-th] (2009)
[5] M. Sinha, B. Mukhopadhyay, A. Sedrakian, *Hypernuclear matter in strong magnetic field*, arXiv:1005.4995 [astro-ph.HE] (2010)
[6] I.A. Shovkoy, *Magnetic Catalysis: A review*, arXiv:1207.5081v2 [hep-ph] (2012)
[7] D. Ebert, K.G. Klimenko, M.A. Vdovichenko, A.S. Vshivtsev, *Magnetic Oscillations in Dense Cold Quark Matter with Four-Fermion Interactions*, arXiv:hep-ph/9905253 (1999)
[8] F. Bruckman, G. Endrodi, T. G. Kovacs, *Inverse magnetic catalysis in QCD*, arXiv:1311.3178v1 [hep-lat] (2013)
[9] E. S. Fraga, B. W. Mintz, J. Schaffner-Bielich, *A search for inverse magnetic catalysis in thermal quark-meson models*, arXiv:1311.3964v1 [hep-ph] (2013)
[10] Michael Kachelriess: *From the Hubble to the Planck Scale: An Introduction to Quantum Fields* (http://web.phys.ntnu.no/ mika/cpp1.16.pdf) (2015)
[11] W.-M. Yao et al. (Particle Data Group), J. Phys. G 33, 1 (2006) G. 't Hooft, M. Veltman, *Regularization and renormalization of gauge fields*, Nuclear Physics B 44 (1): 189–213 (1972)
[12] A. Khodjamirian, *Quantum Chromodynamics and Hadrons: an Elementary Introduction*, arXiv:hep-ph/0403145 (2004)
[13] B.L. Ioffe, *Axial anomaly: the modern status*, Int.J.Mod.Phys.A21:6249-6266,2006
[14] M. G. Alford, K. Rajagopal, T. Schaefer, A. Schmitt, *Color superconductivity in dense quark matter*, arXiv:0709.4635 [hep-ph] (2007)
[15] K. Rajagopal and F. Wilczek, *The condensed matter physics of QCD*, arXiv:hep-ph/0011333.
[16] H. Yukawa, Proc. Phys.-Math. Soc. Jpn, 17, 48 (1935)
[17] B-J. Schaefer, J.M. Pawlowski, J. Wambach, *The Phase Structure of the Polyakov Quark-Meson Model*, arXiv:0704.3234 [hep-ph] (2007)
[18] A. Goyal, M. Dahiya, *Chiral symmetry in linear Sigma model in magnetic environment*, arXiv:hep-ph/9906367 (1999)
[19] C. Itzykson, J. Zuber, *Quantum Field Theory*, p. 543
[20] J.O. Andersen, W.R. Naylor, A. Tranberg, *Phase diagram of QCD in a magnetic field*, Rev. Mod. Phys. 88, 025001 (2016)
[21] A. Heinz, S. Struber, F. Giacosa, D.H. Rischke, *Role of the tetraquark in the chiral phase transition*, arXiv:0805.1134 [hep-ph]
[22] M. E. Peskin, D. V. Schroeder, *An Introduction to quantum field theory* (1997)
[23] L. R. Baboukhadia, V. Elias, M. D. Scadron, *Linear Sigma Model Linkage with Nonperturbative QCD*, arXiv:hep-ph/9708431 (1997)
[24] M. D. Scadron, F. Kleefeld, G. Rupp, *Constituent and current quark masses at low chiral energies*, arXiv:0710.2273 [hep-ph] (2007)
[25] CP-PACS Collaboration, *Phase structure and critical temperature of two-flavor QCD with a renormalization group improved gauge action and clover improved Wilson quark action*, arXiv:hep-lat/0008011 (2000)
[26] Wuppertal-Budapest Collaboration, *Transition temperature and the equation of state from lattice QCD, Wuppertal-Budapest results*, arXiv:1109.5032 [hep-lat] (2011)
[27] Y. Aoki, Sz. Borsanyi, S. Durr, Z. Fodor, S.D. Katz, S. Krieg, K.K. Szabo, *The QCD transition temperature: results with physical masses in the continuum limit II*, arXiv:0903.4155 [hep-lat] (2009)
[28] C.S. Fischer, J. Luecker, J.A. Mueller, *Chiral and deconfinement phase transitions of two-flavour QCD at finite temperature and chemical potential*, arXiv:1104.1564 [hep-ph] (2011)

Appendix A. sums and integrals

Divergent loop integrals are computed using dimensional regularization, setting

$$\int \frac{\mathrm{d}^4\mathbf{k}}{(2\pi)^4} \to \frac{\mathrm{e}^{\gamma_E}}{4\pi}\Lambda^{4-d}\int \frac{\mathrm{d}^d\mathbf{k}}{(2\pi)^d} \tag{A.1}$$

where the renormalization scale Λ has dimension mass and is introduced to preserve the dimension of the integral as the dimension d is varied. The first integral we need is the following:

$$I_1(m^2) = \int \frac{\mathrm{d}k}{2\pi}\sqrt{m^2+k^2}, \tag{A.2}$$

Let

$$I_1 \to \Lambda^{1-d}\int \frac{\mathrm{d}^d\mathbf{k}}{(2\pi)^d}\sqrt{m^2+\mathbf{k}^2}, \tag{A.3}$$

By analytic continuation, we promote the dimension to a continuous variable, setting $d = 1-2\varepsilon$, and view the original integral as (A.3) in the limit $\varepsilon \to 0$. Carrying out the angular part of the integral yields

$$I_1 = \frac{S_{d-1}}{(2\pi)^d}\Lambda^{2\varepsilon}\int_0^\infty \mathrm{d}k k^{d-1}\sqrt{m^2+k^2}, \tag{A.4}$$

where S_{d-1} is the surface area of a unit sphere in d-dimensional space, given by

$$S_{d-1} = \frac{2\pi^{\frac{d}{2}}}{\Gamma\left(\frac{d}{2}\right)}. \tag{A.5}$$

With $k^2 = m^2 t$, the integral takes the form

$$I_1 = \frac{S_{-2\varepsilon}}{(2\pi)^{1-2\varepsilon}}\frac{1}{2}m^2\left(\frac{\Lambda^2}{m^2}\right)^{\varepsilon}\int_0^\infty \mathrm{d}t t^{-\frac{1}{2}-\varepsilon}\sqrt{t+1} \tag{A.6}$$

The integral over t can be computed using an integral representation of Euler's beta function,

$$B(x,y) = \frac{\Gamma(x)\Gamma(y)}{\Gamma(x+y)} = \int_0^\infty \mathrm{d}t \frac{t^{x-1}}{(1+t)^{x+y}}, \tag{A.7}$$

where Γ is the gamma function. We will need the following results:

$$\Gamma\left(-\frac{1}{2}\right) = -2\sqrt{\pi}, \tag{A.8}$$

$$\Gamma(-1+\varepsilon) = -\frac{1}{\varepsilon} + \gamma_E - 1 + \mathscr{O}(\varepsilon), \tag{A.9}$$

where $\gamma_E \approx 0.578$ is the Euler-Mascheroni constant. This yields,

$$\begin{aligned} I_1 &= \frac{1}{2}m^2\left(\frac{\Lambda^2}{m^2}\right)^{\varepsilon}\frac{S_{-2\varepsilon}}{(2\pi)^{1-2\varepsilon}}\int \mathrm{d}t \frac{t^{-\frac{1}{2}-\varepsilon}}{(1+t)^{-\frac{1}{2}}} \\ &= \frac{1}{2}m^2\left(\frac{\Lambda^2}{m^2}\right)^{\varepsilon}\frac{2\pi^{\frac{1}{2}-\varepsilon}}{(2\pi)^{1-2\varepsilon}\Gamma\left(\frac{1}{2}-\varepsilon\right)}\frac{\Gamma\left(\frac{1}{2}-\varepsilon\right)\Gamma(-1+\varepsilon)}{\Gamma\left(-\frac{1}{2}\right)} \\ &= -\frac{m^2}{4\pi}\left(\frac{4\pi\Lambda^2}{m^2}\right)^{\varepsilon}\Gamma(-1+\varepsilon). \end{aligned} \tag{A.10}$$

Expanding in ε,

$$I_1 = -\frac{m^2}{4\pi}\left[1+\varepsilon\ln\left(\frac{4\pi\Lambda^2}{m^2}\right)+\mathscr{O}(\varepsilon^2)\right]\left[-\frac{1}{\varepsilon}+\gamma_E-1+\mathscr{O}(\varepsilon)\right]$$
$$= \frac{m^2}{4\pi}\left[\frac{1}{\varepsilon}+\ln\left(\frac{4\pi\Lambda^2}{m^2}\right)-\gamma_E+1+\mathscr{O}(\varepsilon)\right]. \tag{A.11}$$

Finally, we will make the conventional rescaling

$$\Lambda^2 \to \frac{e^{\gamma_E}}{4\pi}\Lambda^2, \tag{A.12}$$

characterizing the so-called modified minimal subtraction ($\overline{\text{MS}}$) scheme. This gives

$$I_1 = \frac{m^2}{4\pi}\left[\frac{1}{\varepsilon}+\ln\left(\frac{\Lambda^2}{m^2}\right)+1\right]+\mathscr{O}(\varepsilon). \tag{A.13}$$

The second integral we encounter is the following:

$$I_2(m^2) = \int \frac{d^dk}{(2\pi)^d}\frac{1}{k^2-m^2}, \tag{A.14}$$

where k is a Minkowski four-vector. After performing a Wick rotation of the time axis, the integral reads

$$I_2(m^2) = -i\int \frac{d^dk}{(2\pi)^d}\frac{1}{k^2+m^2}, \tag{A.15}$$

with k now a Euclidean vector. This integral can be evaluated in exactly the same way as the previous one:

$$I_2 \to -i\Lambda^{2\varepsilon}\frac{S_{d-1}}{(2\pi)^d}\int_0^\infty \frac{k^{d-1}}{k^2+m^2} \tag{A.16}$$
$$= -i\Lambda^{2\varepsilon}\frac{S_{d-1}}{(2\pi)^d}\frac{1}{2}m^{d-2}\int_0^\infty dt\,\frac{t^{\frac{d}{2}-1}}{1+t} \tag{A.17}$$
$$= -\frac{i}{2}m^2\frac{2\pi^{2-\varepsilon}}{(2\pi)^{4-2\varepsilon}\Gamma(2-\varepsilon)}\left(\frac{\Lambda^2}{m^2}\right)^\varepsilon\frac{\Gamma(2-\varepsilon)\Gamma(-1+\varepsilon)}{\Gamma(1)} \tag{A.18}$$
$$= -\frac{i}{(4\pi)^2}m^2\left(\frac{4\pi\Lambda^2}{m^2}\right)^\varepsilon\Gamma(-1+\varepsilon) \tag{A.19}$$
$$\to \frac{i}{(4\pi)^2}m^2\left(\frac{1}{\varepsilon}+\ln\frac{\Lambda^2}{m^2}+1\right)+\mathscr{O}(\varepsilon). \tag{A.20}$$

The last integral we need is

$$I_3(p^2,m^2) = \int \frac{d^4q}{(2\pi)^4}\frac{1}{[(q+p)^2-m^2]\,[q^2-m^2]}. \tag{A.21}$$

We use the Feynman trick,

$$\frac{1}{ab} = \int_0^1 dz\frac{1}{[az+b(1-z)]^2}. \tag{A.22}$$

The denominator becomes

$$\left[(q^2+2pq+p^2-m^2)z+(q^2-m^2)(1-z)\right]^2=\left[q^2+(2pq+p^2)z-m^2\right]^2=(k^2-M^2)^2, \tag{A.23}$$

where we defined

$$\begin{aligned} k &= q+pz, \\ M^2 &= m^2-p^2z(1-z). \end{aligned} \tag{A.24}$$

After a Wick rotation, we then have

$$I_3(p^2,m^2)=i\Lambda^{2\varepsilon}\int_0^1 \mathrm{d}z\int\frac{\mathrm{d}^dq}{(2\pi)^d}\frac{1}{(q^2+M^2)^2}. \tag{A.25}$$

The integral over q is of the same form as the previous two, and following the same method as before yields

$$\begin{aligned} I_3(p^2,m^2) &= \int_0^1 \mathrm{d}z\frac{i}{(4\pi)^2}\left(\frac{\Lambda^2}{M^2}\right)^{\varepsilon}\left[\frac{1}{\varepsilon}+\mathscr{O}(\varepsilon)\right]=\frac{i}{(4\pi)^2}\left[\frac{1}{\varepsilon}+\log\left(\frac{\Lambda^2}{m_q^2}\right)-\int_0^1 \mathrm{d}z\log\left(\frac{M^2}{m_q^2}\right)+\mathscr{O}(\varepsilon)\right] \\ &= \frac{i}{(4\pi)^2}\left[\frac{1}{\varepsilon}+\log\left(\frac{\Lambda^2}{m_q^2}\right)+F(p^2,m_q^2)+\mathscr{O}(\varepsilon)\right], \end{aligned} \tag{A.26}$$

where

$$F(p^2,m^2)=-\int_0^1 \mathrm{d}z\log\left[1-\frac{p^2}{m^2}z(1-z)\right]=2-2q\,\mathrm{arctan}\frac{1}{q}, \tag{A.27}$$

with

$$q=\sqrt{\frac{4m^2}{p^2}-1}. \tag{A.28}$$

We will also need the derivative of I_3 with respect to p^2. This is given by

$$\frac{\partial}{\partial p^2}I_3(p^2m^2)=\frac{i}{(4\pi)^2}F^{(1)}(p^2,m^2)=\frac{i}{(4\pi)^2}\frac{4m^2q}{p^2(4m^2-p^2)}\mathrm{arctan}\frac{1}{q}-\frac{1}{p^2} \tag{A.29}$$

Hereafter we will use the shorthand $I_1=I_1(m_q^2)$, $I_2(p^2)=I_2(p^2,m_q^2)$ and $F(p^2)=F(p^2,m_q^2)$.

Appendix A.1. Matsubara sums

We need the following two sums:

$$S_1=\sum_{n=-\infty}^{\infty}\ln\left[(\omega_n+i\mu)^2+\omega_{\mathbf{k}}^2\right], \tag{A.30}$$

where $\omega_n=(2n+1)\pi/\beta$, and $S2$ which has the same form, but with $\omega_n=2n\pi$. We will first compute S_1. We have

$$\tanh\left(\frac{z}{2}\right)=\sum_{n=-\infty}^{\infty}\frac{2z}{z^2+(2n+1)^2\pi^2}. \tag{A.31}$$

For $\mu = 0$ this gives directly

$$\frac{\partial}{\partial \omega_{\mathbf{k}}} \sum_n \ln(\omega_n^2 + \omega_{\mathbf{k}}^2) = \sum_n \frac{2\omega_{\mathbf{k}}}{\omega_n^2 + \omega_{\mathbf{k}}^2} = \beta \tanh\left(\frac{\beta \omega_{\mathbf{k}}}{2}\right). \tag{A.32}$$

For $\mu \neq 0$ the sum can be evaluated using the following method. We define

$$f(z) = \frac{2\omega_{\mathbf{k}}}{\omega_{\mathbf{k}}^2 - (z-\mu)^2}, \tag{A.33}$$

$$g(z) = \frac{\beta}{2} \tanh\left(\frac{\beta z}{2}\right) = \sum_{n=-\infty}^{\infty} \frac{z}{z^2 + \omega_n^2} \tag{A.34}$$

As is clear from (145), $g(z)$ has simple poles with residue 1 at $z = i\omega_n$ for all $n \in \mathbb{Z}$, and is analytic everywhere else. Using the residue theorem,

$$\frac{\partial S_1}{\partial \omega_{\mathbf{k}}} = \sum_{n=-\infty}^{\infty} \frac{2\omega_{\mathbf{k}}}{\omega_{\mathbf{k}}^2 + \omega_n^2} = \sum_{n=\infty}^{\infty} f(i\omega_n) = \sum_{z=i\omega_n} Res[f(z)g(z)] = \frac{1}{2\pi i} \oint_C f(z)g(z), \tag{A.35}$$

where C is a contour enclosing the imaginary axis. Since $f(z)g(z)$ falls off faster than $1/z$, this contour can be replaced by two clockwise contours as shown in figure A.17, where the semicircular parts give vanishing contributions to the integrals when the radius is sent to infinity. $f(z)$ has two poles in the area enclosed by these contours: at $z = \mu \pm \omega_{\mathbf{k}}$, with residues -1 and 1.

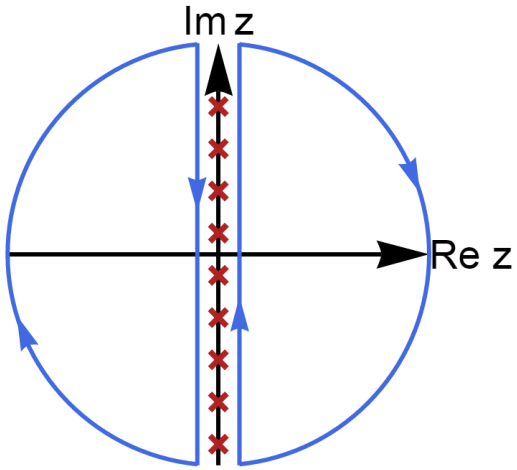

Figure A.17: This integration contour, with the radius of the semicircles taken to infinity, can replace a counterclockwise contour "enclosing" the imaginary axis, if the integrand falls off more rapidly than $\frac{1}{|z|}$.

$$\frac{\partial S_1}{\partial \omega_{\mathbf{k}}} = -\sum_{z=\mu\pm\omega_{\mathbf{k}}} Res[fg(z)] = g(\mu+\omega_{\mathbf{k}}) - g(\mu-\omega_{\mathbf{k}}) = \frac{\beta}{2}\left[\tanh\frac{\beta(\omega_{\mathbf{k}}+\mu)}{2} + \tanh\frac{\beta(\omega_{\mathbf{k}}-\mu)}{2}\right] \tag{A.36}$$

This can be integrated:

$$\begin{aligned}\int d\omega_{\mathbf{k}} \frac{\partial S_1}{\partial \omega_{\mathbf{k}}} &= \ln\left\{\cosh\left[\frac{\beta}{2}(\omega_{\mathbf{k}}-\mu)\right]\right\} + \ln\left\{\cosh\left[\frac{\beta}{2}(\omega_{\mathbf{k}}+\mu)\right]\right\} + \text{constant} \\ &= \beta\omega_{\mathbf{k}} + \ln\left[1+e^{-\beta(\omega_{\mathbf{k}}-\mu)}\right] + \ln\left[1+e^{-\beta(\omega_{\mathbf{k}}+\mu)}\right] + \text{constant},\end{aligned} \tag{A.37}$$

S_2 can be computed in the same way, using

$$\coth(z) = \sum_{n=-\infty}^{\infty} \frac{z}{(\pi n)^2 + z^2}, \tag{A.38}$$

and setting

$$g(z) = \frac{\beta}{2} \coth\left(\frac{\beta z}{2}\right) = \sum_{n=-\infty}^{\infty} \frac{z}{z^2 + \omega_n^2}. \tag{A.39}$$

This gives

$$\frac{\partial S_2}{\partial \omega_{\mathbf{k}}} = \frac{\beta}{2}\left[\coth\frac{\beta(\omega_{\mathbf{k}} + \mu)}{2} + \coth\frac{\beta(\omega_{\mathbf{k}} - \mu)}{2}\right] \tag{A.40}$$

$$\implies S_2 = \beta\omega_{\mathbf{k}} + \ln\left(1 - \mathrm{e}^{-\beta(\omega_{\mathbf{k}}+\mu)}\right) + \ln\left(1 - \mathrm{e}^{-\beta(\omega_{\mathbf{k}}-\mu)}\right) + \text{constant}. \tag{A.41}$$